UC Irvine
UC Irvine Previously Published Works

Title

Designing matrix models for fluorescence energy transfer between moving donors and acceptors

Permalink

https://escholarship.org/uc/item/1sp7v20f

Journal

Biophysical Journal, 64(4)

ISSN

0006-3495

Authors

van der Meer, BW

Raymer, MA

Wagoner, SL

et al.

Publication Date

1993-04-01

DOI

10.1016/s0006-3495(93)81490-5

Copyright Information

Peer reviewed

Designing matrix models for fluorescence energy transfer between moving donors and acceptors

B. Wieb Van Der Meer,* Matthew A. Raymer,* Shawn L. Wagoner,* Richard L. Hackney,*
Joseph M. Beechem,‡ and Enrico Gratton§

*Department of Physics and Astronomy, Western Kentucky University, Bowling Green, Kentucky 42101; ‡Department of Molecular Physiology and Biophysics, Vanderbilt University, Nashville, Tennessee 37232; and §Department of Physics and Laboratory for Fluorescence Dynamics, University of Illinois at Urbana, Champaign, Illinois 61801 USA

ABSTRACT A recipe is given for designing theoretical models for donor–acceptor systems in which fluorescence energy transfer and motion takes place simultaneously. This recipe is based on the idea that a system exhibiting both motion and fluorescence energy transfer can be modeled by specifying a number of "states" and the rates of transitions between them. A state in this context is a set of specific coordinates and conditions that describe the system at a certain moment in time. As time goes on, the coordinates and conditions for the system change, and this evolution can be described as a series of transitions from one state to the next. The recipe is applied to a number of example systems in which the donors and/or acceptors undergo either rotational or translational motion. In each example, fluorescence intensities and anisotropies for the donor and acceptor are calculated from solutions of eigensystems. The proposed method allows for analyzing time-resolved fluorescence energy transfer data without restrictive assumptions for motional averaging regimes and the orientation factor. It is shown that the fluorescence quantities depend on the size of the motional step (i.e., on the number of states), only if fluorescence energy transfer occurs. This finding indicates that fluorescence energy transfer studies may reveal whether the dynamics of a system (e.g., a protein) is better described in terms of transitions between a relatively small number of discrete states (jumping) or a large number of dense states (diffusion).

INTRODUCTION

Fluorescence energy transfer (FET; also called resonance, Förster, excitation, or nonradiative energy transfer) is a powerful tool for estimating intra- and intermolecular distances and distance distributions (1–5). The problem is that the efficiency of energy transfer depends not only on the distance but also on the relative orientations of the donor and acceptor (6, 7) and on the rate of motion of the donor and acceptor moieties with respect to each other (6–10). In the analysis of FET data, often assumptions are used on the orientation factor ("kappa-squared"), the motional averaging regime, or both. Ideally, the data should reveal what the average orientation is and how fast the molecules move.

Our goal in the present study is to understand how the fluorescence observables depend on motional parameters while taking the orientation factor completely into account. With a detailed understanding of these interdependencies, it should be possible to analyze a series of fluorescence observables (such as time-resolved fluorescence intensity and anisotropy of the donor, time-resolved fluorescence intensity and anisotropy of the acceptor, both sensitized and direct) in terms of a series of relevant parameters (such as average distance, width of distance distribution, rate of rotational motion, rate of translational motion, orientational parameters).

In this article we are taking a number of initial steps toward this goal by introducing a new approach to designing theoretical models for donor–acceptor systems in which fluorescence energy transfer and motion take place simultaneously. This approach is based on the idea that a system exhibiting both motion and fluorescence energy transfer can be modeled by specifying a number of "states" and the rates of transitions between them. A state in this context is a set of specific coordinates and conditions that describe the system at a certain moment in time. As time goes on, the coordinates and conditions for the system change, and this evolution can be described as a series of transitions from one state to the next. Our method is illustrated by applying it to three systems in which the donors and/or acceptors undergo either rotational or translational motion. In each of these examples, fluorescence intensities and anisotropies for the donor and acceptor are calculated from solutions of eigensystems. The three examples are as follows.

(a) The donor–acceptor distance is fixed. The acceptor has a single transition moment that is oriented along the laboratory z-axis. The donor–acceptor separation vector is also along the z-axis. The donor also has one single transition moment, but this can align with the x-, the y-, or the z-axis. Rotational motion is modeled as transitions between these orientations.

(b) The donor and acceptor are rigidly bound to a spherical molecule. The transition moment of the acceptor cannot move with respect to the molecule, but the whole molecule can rotate in such a way that the acceptor moment is aligned with the x-, the y-, or the z-axis. The donor–acceptor separation vector is parallel to the acceptor moment. The donor can rotate with respect to the molecule, and its moment is oriented along the x-, the y-, or the z-axis. This case can be regarded as a more

Address correspondence to Dr. B. Wieb Van Der Meer, Department of Physics and Astronomy, Western Kentucky University, 1526 Russellville Road, Bowling Green, KY 42101-3576, USA.

M. A. Raymor's and S. L. Wagoner's present address is Department of Physics, North Carolina State University, Raleigh, NC 27695.

realistic modification of the first model. Note that the cases (*a*) and (*b*) for zero transfer reduce to variations of orientational exchange models for fluorescence anisotropy decay introduced by Piston and Gratton (11), and Weber (12).

(*c*) The donor and acceptor are rigidly attached to either end of a linear molecule. The kappa-squared is assumed to be constant because of rapid rotation or degenerate transition moments. The molecule can occupy any of N states, where N is an integer between 2 and 25. These states have different donor–acceptor distances. The internal dynamics of the molecule is modeled by allowing transitions between neighboring states, i.e., states with slightly different molecular length. This case is an alternative for the theory discussed by Haas and co-workers (5, 13).

The outline of the article is as follows. In the next section, we formulate our method as a recipe. Then we show how it works in three examples for FET combined with translational or rotational motion and calculate the time-resolved fluorescence intensities and anisotropies. Details of the derivations, most of which are matrix manipulations, are presented in the Appendices. We compare results for a "small" number of states with those for a "large" number of states. In the case of the third example small means 4 and large implies 20 states, but in the first (second) example, small means 3 (9) states and large refers to an infinite number of states giving rise to a diffusion equation coupled to transfer. These diffusion equations are also solved using matrix methods (see Appendices B and D). In the Discussion we summarize our main findings, one of which is that the observables depend on the size of the motional step, only if FET occurs. This finding indicates that fluorescence energy transfer studies may reveal whether the dynamics of a system (e.g., a protein) are better described in terms of transitions between a number of discrete states or in terms of diffusion equations. This article offers a method for designing models for donor–acceptor systems. The results of such models can then be used for analyzing FET data without restrictive assumptions on motional averaging regimes and kappa-squared. A preliminary account of this work has been published (14).

THEORY

The idealized experimental situation we have in mind is depicted in Figure 1. A flash of vertically polarized light travels along the negative x-direction and excites a sample situated in the origin. The sample contains donors and acceptors. The excited state of the donor depopulates either by radiative decay or by FET. The acceptor can be excited both directly and by transfer from the donor and loses its excitation energy by radiative decay only. Fluorescence emitted by the donor or the acceptor traveling along the y-axis is observed through a vertical or a horizontal polarizer, yielding the vertical or the hori-
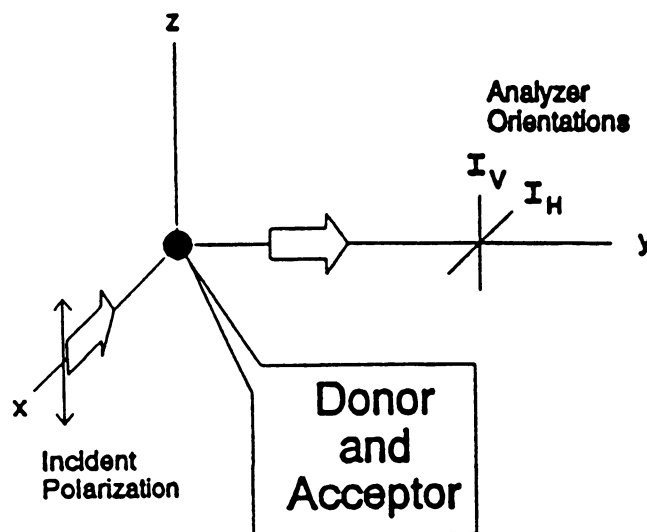

FIGURE 1 Schematics of the experiment to which the theory refers. The laboratory frame is shown with the sample in the origin. The arrow pointing to the origin represents the flash of vertically polarized light that excites the system; the arrow pointing in the y-direction indicates the emission, of which the vertical and the horizontal components (I_V and I_H, respectively) are measured.

zontal component of the fluorescence intensity (I_V or I_H, respectively). We are interested in the fluorescence intensity, $I = I_V + 2I_H$, and the fluorescence anisotropy, $r = (I_V - I_H)/I$, both of the donor and the acceptor. The relevant quantities are I_D, r_D, I_A and r_A, which are defined in Table 1.

Our recipe for model design is as follows.

(*a*) Define the excited-donor states and the probabilities that they are occupied, call these probabilities, e.g., $x_1 \cdots x_N$ (N is the number of states). Define the corresponding excited-acceptor states with the probabilities that these are occupied. These probabilities could be called $y_1 \cdots y_N$. The transfer rates T_1 (from the x_1-state to the y_1-state) up to T_N (from the x_N-state to the y_N-state) can now be derived.

(*b*) Define the motional transitions between the states in terms of parameters, indicating rates of rotation and/or translation.

(*c*) Define fluorescence donor and acceptor decay rates (and related nonradiative rates if needed).

(*d*) Find the time-zero values for $x_1 \cdots x_N$ and $y_1 \cdots y_N$ from the photoselection criterion used (we assumed here that the system is excited by an extremely short flash of vertically polarized light. After finding the fluorescence responses to this type of excitation, it is possible to derive responses to other excitation modes [steady state or harmonic] by convolution.)

(*e*) Express the donor fluorescence intensity and anisotropy in terms of $x_1 \cdots x_N$.

(*f*) Set up the matrix equation for $x_1 \cdots x_N$, find the eigenvalues and eigenvectors, and solve, expressing the donor intensity and anisotropy in terms of the time after

$I_D = I_D(t)$ = the donor intensity at a time t after the flash

$I_{D0} = I_D(0)$ = the donor intensity immediately after the flash

$r_D = r_D(t)$ = the fluorescence anisotropy of the donor

$I_A = I_A(t)$ = the fluorescence intensity of the acceptor

$I_{A0} = I_A(0)$ = the acceptor intensity immediately after the flash at the wavelength where the donor is excited. No transfer has occurred yet; I_{A0} is solely due to direct fluorescence.

$\epsilon = I_{A0}/I_{D0}$ = the ratio of acceptor absorbance times quantum yield over donor absorbance times quantum yield at donor excitation wavelengths. This parameter is used for distinguishing direct and sensitized acceptor fluorescence.

$r_A = r_A(t)$ = the fluorescence anisotropy of the acceptor

the flash, the time-zero values, and the eigenvectors and eigenvalues.

(*g*) Express the acceptor fluorescence intensity and anisotropy in $y_1 \cdots y_N$.

(*h*) Set up the acceptor matrix equation in terms of $y_1 \cdots y_N$, the matrix containing the motional parameters and the decay parameters, and the vector T_1 times $x_1 \cdots T_N$ times x_N and solve expressing the acceptor intensity and anisotropy in terms of the time after the flash, the time-zero values, and the eigenvectors and eigenvalues of the donor matrix and the eigenvalues and eigenvectors of the acceptor matrix. In some cases it is possible to derive a differential equation for the acceptor intensity and solve that equation without solving the matrix equation first.

Below we will introduce three examples of donor-acceptor systems and show how the recipe works. The eigenvalue-eigenvector problem for the first two examples can be solved analytically. For the last example and for solving the diffusion equations (see Appendices E, B, and D), eigenvectors and eigenvalues are obtained numerically using a software package in True Basic using eigenvalue-eigenvector routines from the IMSL libraries (15). A copy of this program is available upon request.

Example 1: an oriented system with rotational motion only

(*a*) The first example is illustrated in Figure 2. The donor has one single transition moment, which can have one out of three possible orientations, corresponding to three states for the excited donor. These states and the correspondent probabilities are $\underline{x}_D$ = state in which the donor moment is aligned with the x-axis; x_D = the probability that $\underline{x}_D$ is occupied; $\underline{y}_D$ = state in which the donor moment is aligned with the y-axis; y_D = the probability that $\underline{y}_D$ is occupied; $\underline{z}_D$ = state in which the donor moment is aligned with the z-axis; and z_D = the probability that $\underline{z}_D$ is occupied. Similarly, the excited-acceptor states and probabilities are $\underline{x}_A$ = state in which the donor mo-

ment is aligned with the x-axis; x_A = the probability that $\underline{x}_A$ is occupied; $\underline{y}_A$ = state in which the donor moment is aligned with the y-axis; y_A = the probability that $\underline{y}_A$ is occupied; $\underline{z}_A$ = state in which the donor moment is aligned with the z-axis; and z_A = the probability that $\underline{z}_A$ is occupied. The excited donor can lose energy by radiative decay or by FET. The rate of transfer is $T \times OF$ where OF is the orientation factor, kappa-squared. The donor-acceptor distance is fixed, so that T is a constant. The acceptor, which also has one single transition moment, has its moment permanently oriented along the laboratory z-axis. As a result, the orientation factor for the state $\underline{z}_D$ equals 4, but is equal to 0 for both $\underline{x}_D$ and $\underline{y}_D$.

(*b*) Rotational motion is modeled by allowing transitions between the states at a rate of $2R$. The origin of the factor 2 in $2R$ and other details of the derivations for this model can be found in Appendix 1.

(*c*) The rate of radiative decay for the donor is k_D. That of the acceptor is k_A.

(*d*) Immediately after the flash, both x_D and y_D equal 0.2 and z_D equals 0.6 (11). In this oriented sample, however, both x_A and y_A equal zero immediately after the flash and z_A equals ϵ, a parameter equal to the ratio of acceptor absorbance times quantum yield over donor absorbance times quantum yield at donor excitation wavelengths.
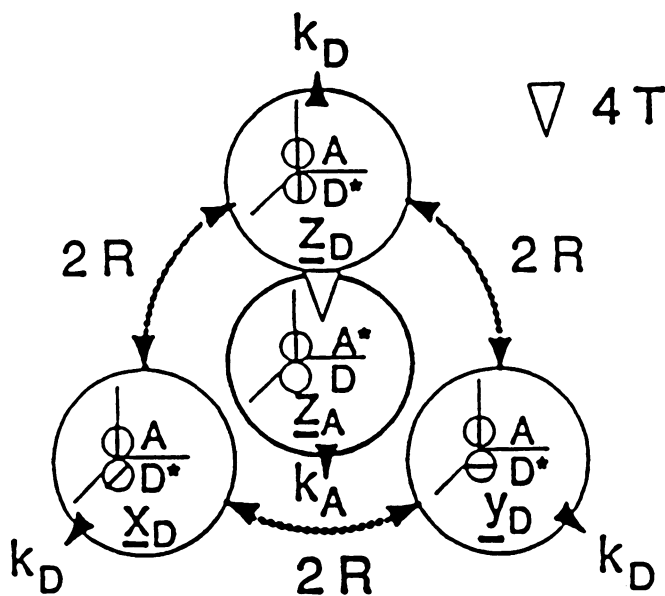

FIGURE 2 Rotational motion only in an oriented system. States for example 1 are shown with the transitions that take place in this model. In the states $\underline{x}_D$, $\underline{y}_D$, and $\underline{z}_D$ (labeled with D*) the donor is excited. The orientation of the donor and acceptor transition moments in these states are indicated. In state $\underline{z}_A$ (labeled with A*) the acceptor is excited. The orientation of its transition moment is shown. R is the rate of 90° rotational jumps, k_D is the rate of radiative decay of the donor, k_A is that of the acceptor, T is the rate of transfer from the donor to the acceptor for the orientation factor equal to unity. In the state $\underline{z}_D$ the orientation factor equals 4; in $\underline{x}_D$ and $\underline{y}_D$ it equals 0.

(e) The fluorescence intensity is given by $I_D = I_{D0}(z_D + 2x_D)$, and the fluorescence anisotropy of the donor equals $r_D = (z_D - x_D)/(z_D + 2x_D)$.

(f) The matrix equation for x_D, y_D, and z_D is represented diagramatically in Figure 2 and is given in Eq. 1:

$$\frac{d}{dt}\begin{pmatrix} x_D \\ y_D \\ z_D \end{pmatrix} = \begin{pmatrix} -a_1 & 2R & 2R \\ 2R & -a_1 & 2R \\ 2R & 2R & -a_2 \end{pmatrix}\begin{pmatrix} x_D \\ y_D \\ z_D \end{pmatrix} \quad (1)$$

$$a_1 = k_D + 4R \quad a_2 = a_1 + 4T.$$

The solution of Eq. 1 is a linear combination of the eigenvectors of the matrix times exponentials of the eigenvalues with coefficients matching time 0 values for the components (see Appendix A). These quantities are given in Eq. (2):

$$I_D = \frac{I_{D0}}{10W}[5W + 15R - 2T + (5W - 15R + 2T)e^{-2Wt}]$$

$$\times e^{-(k_D + 2R + 2T - W)t}, \quad (2a)$$

$$W = \{8R^2 + (R + 2T)^2\}^{1/2}, \quad (2b)$$

$$r_D = [r_{D\infty} + 0.2(1 + 2B - 5r_{D\infty})e^{-2Wt}]/[1 + Be^{-2Wt}], \quad (2c)$$

$$r_{D\infty} = \frac{2W - 6R - 8T}{5W + 15R - 2T} \quad B = \frac{5W - 15R + 2T}{5W + 15R - 2T}. \quad (2d)$$

(g) The acceptor fluorescence is equal to $I_{D0}(z_A + 2x_A)$ and the acceptor anisotropy is $r_A = (z_A - x_A)/(z_A + 2x_A)$. In general, both x_A and z_A contain two terms: one due to transfer from the donor and the other due to direct acceptor excitation.

(h) The matrix equation for the probabilities for the excited acceptor states reads:

$$\frac{d}{dt}\begin{pmatrix} x_A \\ y_A \\ z_A \end{pmatrix} = \begin{pmatrix} -k_A & 0 & 0 \\ 0 & -k_A & 0 \\ 0 & 0 & -k_A \end{pmatrix}\begin{pmatrix} x_A \\ y_A \\ z_A \end{pmatrix} + 4T\begin{pmatrix} 0 \\ 0 \\ z_D \end{pmatrix}. \quad (3)$$

The solution of this equation with the boundary conditions indicated above is derived in Appendix A. From this solution, the acceptor intensity and anisotropy can be calculated:

$$I_A = I_{D0}\{\epsilon e^{-k_A t} + A_A + B_A\}, \quad r_A = 1, \quad (4a)$$

with

$$A_A = 0.4T\left(\frac{3W + R - 6T}{W}\right)$$

$$\times \left\{\frac{e^{-(k_D + 3R + 2T - W)t} - e^{-k_A t}}{k_A - (k_D + 3R + 2T - W)}\right\}, \quad (4b)$$

and

$$B_A = 0.4T\left(\frac{3W - R + 6T}{W}\right)$$

$$\times \left\{\frac{e^{-(k_D + 3R + 2T + W)t} - e^{-k_A t}}{k_A - (k_D + 3R + 2T + W)}\right\}. \quad (4c)$$

Figure 3 illustrates the dependence of the time-resolved Donor fluorescence and anisotropy on the rate of transfer (A and C) and on the rate of rotation (B and D). This three-state model can be generalized by introducing more states and considering the motional transitions between them. As is shown in Appendix B, in the limit of an infinite number of states, the matrix equation becomes a diffusion equation. This equation can be solved by matrix methods as shown in Appendix B. Figure 4 illustrates the dependence of the time-resolved donor fluorescence and anisotropy on the rate of transfer (A and C) and on the rotational diffusion constant (B and D).

Example 2: an isotropic system with two types of rotation

(a) The donor and acceptor are rigidly bound to a spherical molecule. The transition moment of the acceptor cannot reorient with respect to the molecule, but the whole molecule can rotate in such a way that the acceptor moment is aligned with the x-, the y-, or the z-axis. The donor–acceptor separation vector is parallel to the acceptor moment, and the donor–acceptor distance is fixed. The donor can rotate with respect to the molecule, but its moment is oriented either along the x-, the y-, or the z-axis. For the excited donor, there are nine states denoted by ξ_i, where ξ stands for x, y, or z and i for 1, 2, or 3.

The state ξ_i is the state in which the transition moment of the excited donor is aligned with the ξ-axis and the acceptor moment is aligned with the x-axis if i = 1, with the y-axis if i = 2, or with the z-axis if i = 3. The probability that the state ξ_i is occupied is denoted by ξ_i. These states, the transitions between them, and the depopulation modes of the excited donor states are illustrated in Fig. 5. The three excited acceptor states, $\underline{x}_A$, $\underline{y}_A$, and $\underline{z}_A$, in which the acceptor is aligned with the x-, y-, or z-axis, respectively, are shown in Fig. 6. The transitions between them and the (de)population modes of these states are also shown in Fig. 6. The probability that the state $\underline{x}_A$, $\underline{y}_A$, or $\underline{z}_A$ is occupied is x_A, y_A, or z_A, respectively.

(b) The motional transitions are defined in Figures 5 and 6.

(c) The fluorescence donor decay rate is k_D. The fluorescence decay rate for the acceptor is k_A.

(d) A direct extension of the photoselection criterium used by Piston and Gratton (11) leads to the following time 0 values for these variables; $x_1 = y_1 = x_2 = y_2 = x_3 = y_3 = \frac{1}{15}$, $z_1 = z_2 = z_3 = \frac{1}{5}$.

(e) The donor intensity, I_D, and anisotropy, r_D, are given by:

$$I_D = I_{D0}(z_1 + z_2 + z_3 + 2x_1 + 2x_2 + 2x_3).$$

$$r_D = (z_1 + z_2 + z_3 - x_1 - x_2 - x_3)/$$
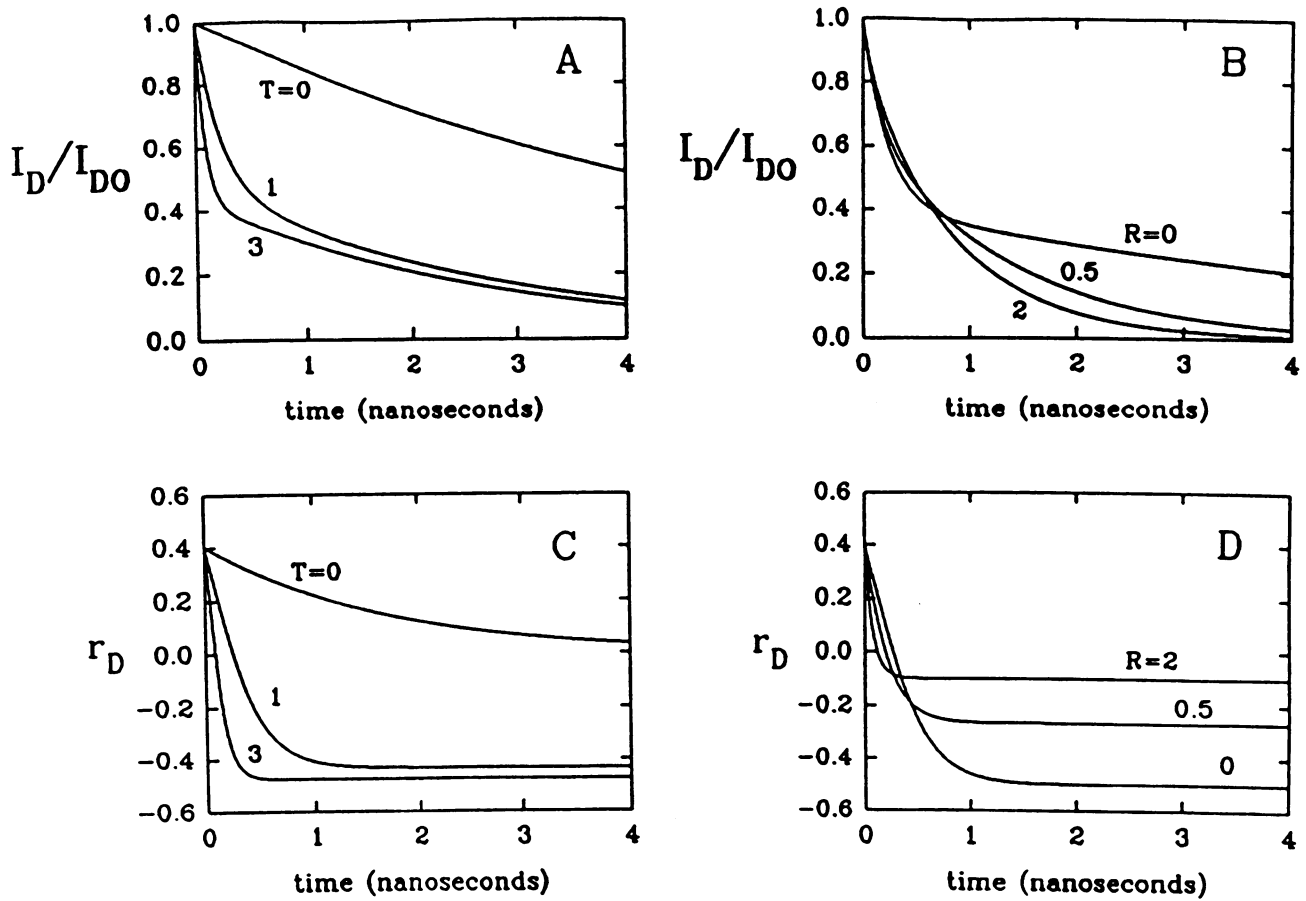
$$(z_1 + z_2 + z_3 + 2x_1 + 2x_2 + 2x_3).$$

FIGURE 3 Rotational motion only in an oriented system. The dependence of the time-resolved donor fluorescence and anisotropy on the rate of transfer and rotation is shown for example 1. T is the rate of transfer from the donor to the acceptor at unit orientation factor, $k_D^{-1} = 6$ ns (k_D is the rate of radiative decay of the donor). Here R denotes the rate of rotational transitions. Compare with Fig. 4, where R is the rotational diffusion constant of the donor, and 6×6 cutoff matrices are used (see Appendix B). (A) Intensity; (C) anisotropy with $R = 0.1$ ns^{-1}, $T = 0$, 1, and 3 ns^{-1}. (B) Intensity; (D) anisotropy with $R = 0$, 0.5, and 2 ns^{-1}, $T = 1$ ns^{-1}.

(f) The set of linear differential equations for the probabilities $\underline{\xi}_i$ ($\xi = x, y, z; i = 1, 2, 3$) corresponding to the transitions and decay modes of Figure 5 can be written as the following matrix equation:

$$\frac{d}{dt}\begin{pmatrix} x_1 \\ y_1 \\ z_1 \\ x_2 \\ y_2 \\ z_2 \\ x_3 \\ y_3 \\ z_3 \end{pmatrix} = \begin{pmatrix} -c_1 & 2R & 2R & 0 & 2R_M & 0 & 0 & 0 & 2R_M \\ 2R & -c_2 & \Pi & 2R_M & 0 & 0 & 0 & 2R_M & 0 \\ 2R & \Pi & -c_2 & 0 & 0 & 2R_M & 2R_M & 0 & 0 \\ 0 & 2R_M & 0 & -c_2 & 2R & \Pi & 2R_M & 0 & 0 \\ 2R_M & 0 & 0 & 2R & -c_1 & 2R & 0 & 0 & 2R_M \\ 0 & 0 & 2R_M & \Pi & 2R & -c_2 & 0 & 2R_M & 0 \\ 0 & 0 & 2R_M & 2R_M & 0 & 0 & -c_2 & \Pi & 2R \\ 0 & 2R_M & 0 & 0 & 0 & 2R_M & \Pi & -c_2 & 2R \\ 2R_M & 0 & 0 & 0 & 2R_M & 0 & 2R & 2R & -c_1 \end{pmatrix} \begin{pmatrix} x_1 \\ y_1 \\ z_1 \\ x_2 \\ y_2 \\ z_2 \\ x_3 \\ y_3 \\ z_3 \end{pmatrix}$$

$$c_1 = k_D + 4R + 4R_M + 4T \qquad c_2 = k_D + 4R + 6R_M \qquad \Pi = 2(R + R_M). \tag{5}$$

The solution of Eq. 5 corresponding to the boundary condition given above yields the following expressions for the donor intensity, I_D, and anisotropy, r_D (see Appendix C):

$$I_D = I_{D0}e^{-(3R+2T+k_D)t}[(3W + 9R + 2T)e^{+Wt} + (3W - 9R - 2T)e^{-Wt}]/[6W], \tag{6a}$$

$$r_D = [r_L + 0.2e^{-2Wt} + (r_L + 0.2)e^{-W+3R-2T)t}]e^{-6R_Mt}/ [1 + 5r_Le^{-2Wt}], \tag{6b}$$

$$r_L = (3W - 9R - 2T)/(15W + 45R + 10T). \tag{6c}$$

Figure 7 illustrates the dependence of the time-resolved donor intensity and anisotropy on the rate of
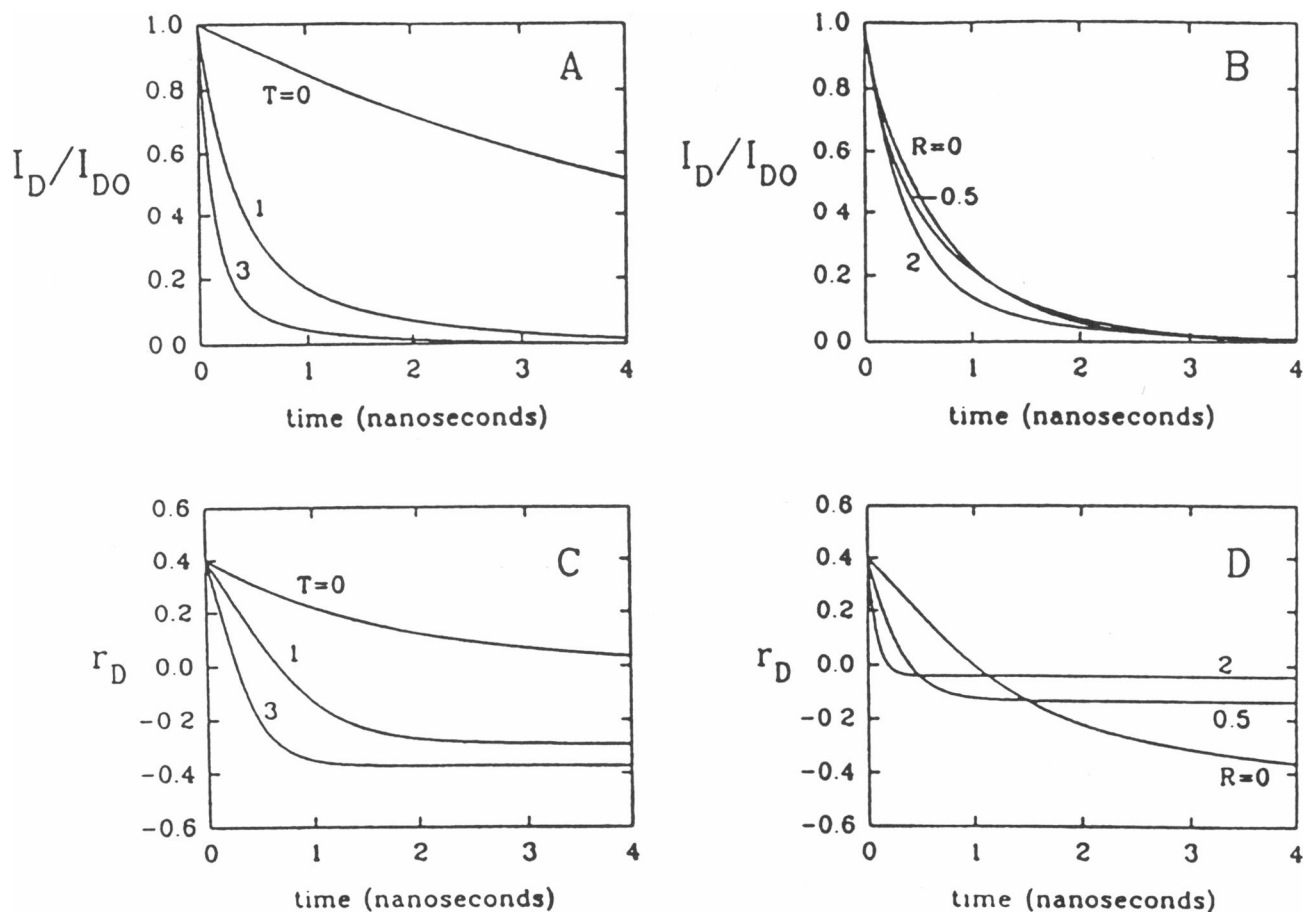
FIGURE 4 Profile of an oriented system, per Fig. 3, with these exceptions: here R is the rotational diffusion constant of the donor, and 6×6 cutoff matrices are used (see Appendix B).

transfer and the rate of donor rotation. This nine-state model can be generalized by introducing more states and considering the motional transitions between them. Again, in the limit of an infinite number of states, the matrix equation becomes a diffusion equation. This equation can be solved by matrix methods as shown in Appendix D. Figure 8 illustrates the dependence of the time-resolved donor fluorescence and anisotropy on the

rate of transfer (A and C) and on the rotational diffusion constant (B and D).

(g) The acceptor fluorescence is equal to $I_{D0}(z_A + 2x_A)$, and the acceptor anisotropy is $r_A = (z_A - x_A)/(z_A + 2x_A)$. In general, both x_A and z_A contain two terms: one due to transfer from the donor and the other due to direct acceptor excitation.

(h) The matrix equation for the acceptor probabilities reads,

$$\frac{d}{dt}\begin{pmatrix} x_A \\ y_A \\ z_A \end{pmatrix} = \begin{pmatrix} -(k_A + 4R_M) & 2R_M & 2R_M \\ 2R_M & -(k_A + 4R_M) & 2R_M \\ 2R_M & 2R_M & -(k_A + 4R_M) \end{pmatrix}\begin{pmatrix} x_A \\ y_A \\ z_A \end{pmatrix} + 4T\begin{pmatrix} x_1 \\ y_2 \\ z_3 \end{pmatrix}. \tag{7}$$

The fluorescence intensity and anisotropy of the acceptor is derived from the solution of Eq. 7 with this boundary condition in Appendix C, and reads,

$$I_A = I_{D0}e^{-k_A t}\left\{\epsilon + \frac{2T}{3W}(W + 3R - 2T)P_A + \frac{2T}{3W}(W - 3R + 2T)M_A\right\}, \tag{8a}$$

$$r_A = 0.4e^{-6R_M t}\left\{\frac{\epsilon + \frac{2T}{3W}(W - 3R - 2T)P_A + \frac{2T}{3W}(W + 3R + 2T)M_A}{\epsilon + \frac{2T}{3W}(W + 3R - 2T)P_A + \frac{2T}{3W}(W - 3R + 2T)M_A}\right\}, \tag{8b}$$

$$P_A = \frac{e^{(k_A - k_D - 3R - 2T + W)t} - 1}{k_A - k_D - 3R - 2T + W} \qquad M_A = \frac{e^{(k_A - k_D - 3R - 2T - W)t} - 1}{k_A - k_D - 3R - 2T - W}. \tag{8c}$$

$\longleftrightarrow$ 2 R$_M$

$\longleftarrow \cdots \cdots \rightarrow$ 2 R
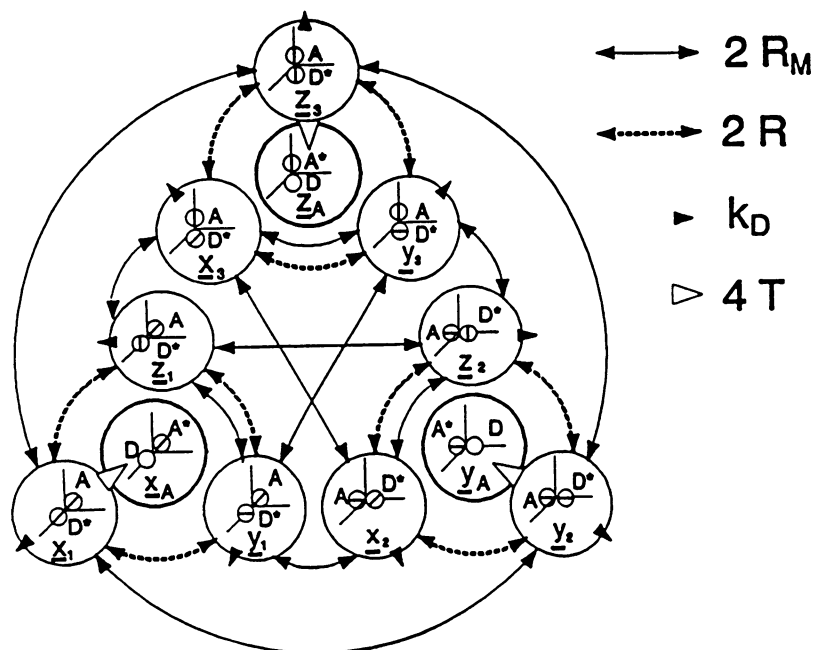
$\blacktriangleright$ k$_D$

$\triangleright$ 4 T

FIGURE 5 Rotational motion only in an isotropic system. The excited donor states of example 2 (labeled with D*), x_i, y_i, and z_i (i = 1, 2, 3) are shown with their donor and acceptor moments (lines in the dumbbells). The transitions between these states are also indicated. These are due to molecular rotations at a rate R_M and intermolecular donor rotations at a rate R. The nonradiative decay at rate k_D as well as transfer are denoted. The rate of transfer to excited acceptor states (also shown, labeled with A*), z_A, x_A, or y_A, is nonzero only for the transitions x_1 to x_A, y_2 to y_A, and z_3 to z_A, and this rate constant is equal to $4T$. The direction of the acceptor transition moments of the excited acceptor states are also shown.

Figure 9 illustrates the time dependence of the acceptor intensity and anisotropy of the acceptor for different values of the rate of transfer. Figure 10 pictures the dependence of the acceptor intensity and anisotropy on time and rate of transfer in the case of diffusion.

Example 3: translational motion only

(a) The donor and acceptor are rigidly attached to either end of a linear molecule. The kappa-squared is assumed to be two-thirds, and both donor and acceptor
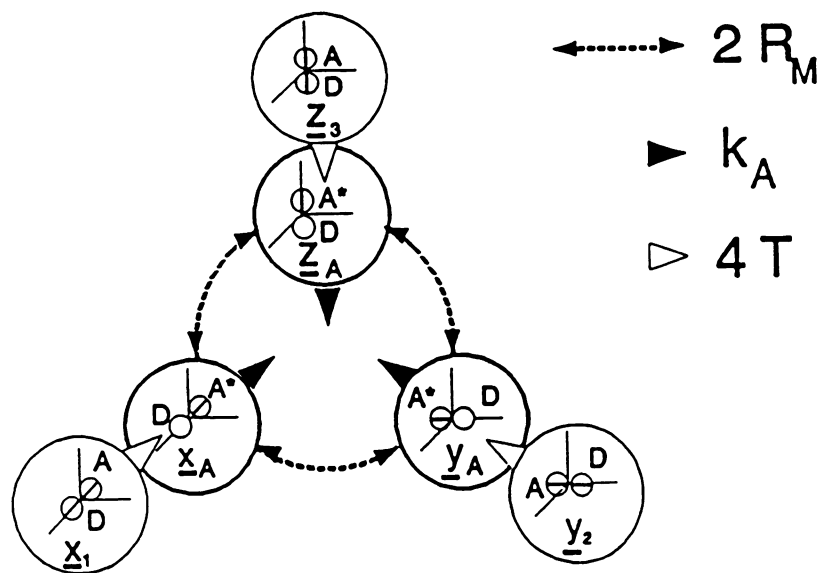

$\longleftarrow \cdots \cdots \rightarrow$ 2 R$_M$

$\blacktriangleright$ k$_A$

$\triangleright$ 4 T

FIGURE 6 Rotational motion only in an isotropic system. The excited acceptor states x_A, y_A, and z_A for example 2 are illustrated with the transitions between each other due to molecular rotations at a rate R_M. The transfer transitions from x_1 to x_A, from y_2 to y_A, and from z_3 to z_A at a rate $4T$ are also shown as well as the radiative decay transitions at a rate k_A.
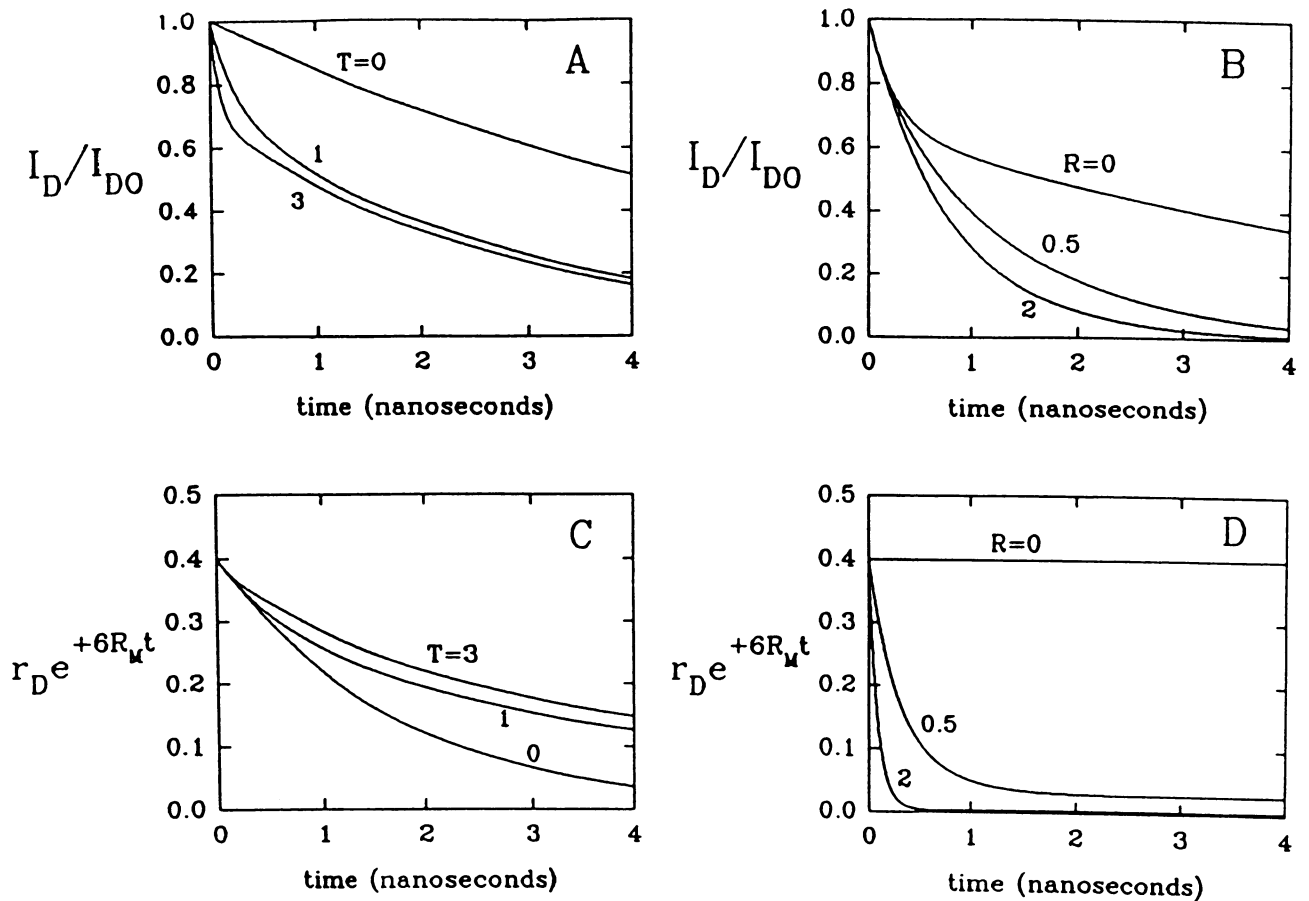
FIGURE 7 Rotational motion only in an isotropic system. The dependence of the time-resolved donor fluorescence and anisotropy on the rate of transfer and rotation is shown for example 2. T is the rate of transfer from the donor to the acceptor at unit orientation factor, $k_D^{-1} = 6$ ns (k_D is the rate of radiative decay of the donor). Here R and R_M denote rotational rate constants for the donor and the whole molecule, respectively. Compare with Fig. 8, where R is the rotational diffusion constant for the donor within the molecule, and R_M is the rotational diffusion constant for the whole molecule, and the size of the cutoff matrices is 11×11 (see Appendix D). (A) Intensity; (C) anisotropy with $R = 0.1$ ns^{-1}, $T = 0$, 1, and 3 ns^{-1}. (B) Intensity; and (D) anisotropy with $R = 0, 0.5$, and 2 ns^{-1}, $T = 1$ ns^{-1}. The anisotropy does not depend on R_M except for a factor $\exp(-6R_M t)$. The anisotropy divided by this factor is plotted in Figs. 7, C and D, and 8, C and D.

are isotropic with vanishing fluorescence anisotropy. The molecule can occupy any of N ($N = 2, \ldots, 25$) states with different donor–acceptor distances. The internal dynamics of the molecule is modeled by allowing transitions between neighboring states, i.e., states with slightly different molecular length, as illustrated in Figure 11. This model is similar to a compartmental version of the model discussed in references 5 and 13. There are N possible states for excited donors, where N is an integer between 2 and 25. The shortest donor–acceptor distance is denoted by s, and this is the donor–acceptor distance for the state 1. The medium distance is a. In state N the molecular length equals $2a - s$, the largest possible distance. The other states have a length equally spaced between these extremes, so that r_m, the donor–acceptor distance for state m ($m = 1, \ldots, N$), is given by:

$$r_m = \frac{2(m-1)}{N-1} a + \frac{N-2m+1}{N-1} s \qquad (9)$$

Let $x_m = x_m(t)$ be the fraction of molecules in state m ($m = 1, \ldots, N$) having a donor–acceptor distance r_m at time t after the flash. There are also N excited acceptor states. Let $y_m = y_m(t)$ denote the fraction of molecules having the acceptor excited and a donor–acceptor distance equal to r_m ($m = 1 \cdots N$). The rate of transfer, T_m, in state m depends on the donor–acceptor distance for that state according to Förster's distance law:

$$T_m = k_D \frac{R_0^6}{r_m^6}, \qquad (10)$$

where R_0 denotes the Förster distance.

(b) Internal dynamics is modeled by allowing transitions from state m to state m + 1 ($m = 1 \cdots N - 1$) at a rate $J_{m,m+1}$ and from state m + 1 to state m ($m = 1 \cdots N - 1$) at a rate $J_{m+1,m}$. To assure that at equilibrium the net number of transitions from m to m + 1 equals that from m + 1 to m, we must have that

$$J_{m,m+1} \times x_m(0) = J_{m+1,m} \times x_{m+1}(0). \qquad (11)$$
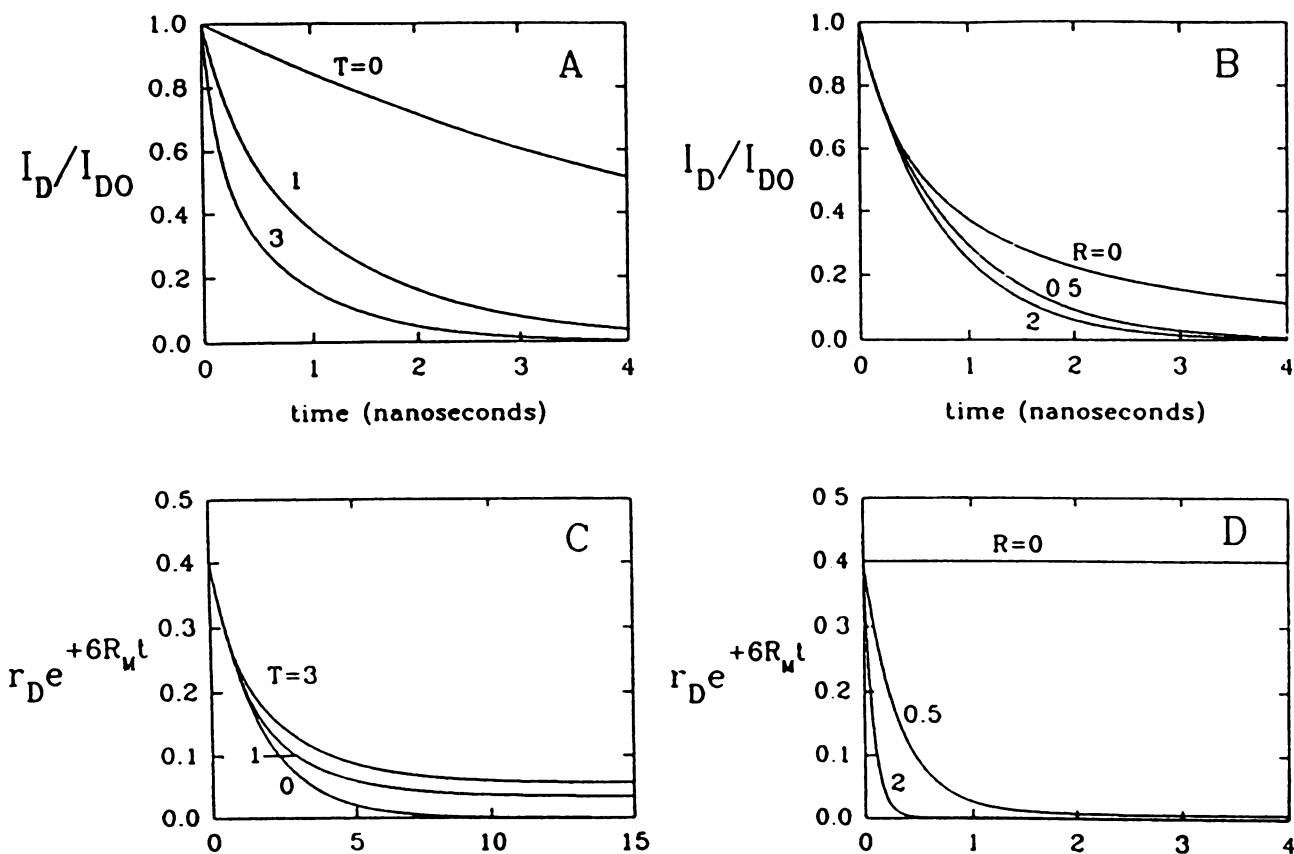
FIGURE 8 Profile of an isotropic system, per Fig. 7, with these exceptions: here R is the rotational diffusion constant for the donor within the molecule and R_M is the rotational diffusion constant for the whole molecule. Here the size of the cutoff matrices is 11×11 (see Appendix D).

(c) The donor fluorescence decay rate is k_D, and that of the acceptor is k_D.

(d) The distribution of states immediately after the flash is the equilibrium distribution, assumed to be a Gaussian with width σ, i.e., for m = $1 \cdots N$, the time 0 values for $x_1 \cdots x_N$ and $y_1 \cdots y_N$ are given by:

$$x_m(0) = e^{-p_m} \Big/ \sum_{m=1}^{N} e^{-p_m} \quad \text{and}$$

$$y_m(0) = \epsilon x_m(0) \quad \text{for} \quad m = 1 \cdots N, \tag{12}$$

with

$$p_m = \frac{(r_m - a)^2}{2\sigma^2} = \frac{1}{2}\left[\left(\frac{a-s}{\sigma}\right)\left(\frac{2m - N - 1}{N - 1}\right)\right]^2. \tag{13}$$

(e) The intensity of the donor fluorescence is proportional to the sum of all the fractions of molecules with an excited donor:

$$I_D = I_{DO} \sum_{m=1}^{N} x_m. \tag{14}$$

The donor anisotropy vanishes at all times since the donor fluorophore (and also the acceptor fluorophore) is assumed to be intrinsically isotropic.

(f) The rate equations for the fractions x_m (m = $1 \cdots N$) in the case $N = 4$ can be written as:

$$\frac{d}{dt}\begin{pmatrix} x_1 \\ x_2 \\ x_3 \\ x_4 \end{pmatrix} = \begin{pmatrix} -e_1 & Je^{-p_1} & 0 & 0 \\ Je^{-p_2} & -e_2 & Je^{-p_2} & 0 \\ 0 & Je^{-p_3} & -e_3 & Je^{-p_3} \\ 0 & 0 & Je^{-p_4} & -e_4 \end{pmatrix}\begin{pmatrix} x_1 \\ x_2 \\ x_3 \\ x_4 \end{pmatrix} \tag{15}$$

$$e_1 = k_D + T_1 + Je^{-p_2}$$

$$e_2 = k_D + T_2 + J(e^{-p_1} + e^{-p_3})$$

$$e_3 = k_D + T_1 + J(e^{-p_2} + e^{-p_4})$$

$$e_4 = k_D + T_1 + Je^{-p_3},$$

where k_D is the rate of radiative donor decay and J is a rate constant independent of m, defined as $J = e^{p_{m+1}}J_{m,m+1} = e^{p_m}J_{m+1,m}$. The general matrix equation for $N = 2 \cdots 25$ is given in Appendix E. For comparing results for different N, we define the lateral diffusion constant D_L as:

$$D_L = Jd^2, \tag{16}$$

where d equals $|r_m - r_{m+1}| = 2(a - s)/(N - 1)$. Again, the solution of the matrix equation is a linear combination of eigenvectors times exponentials of the eigen-
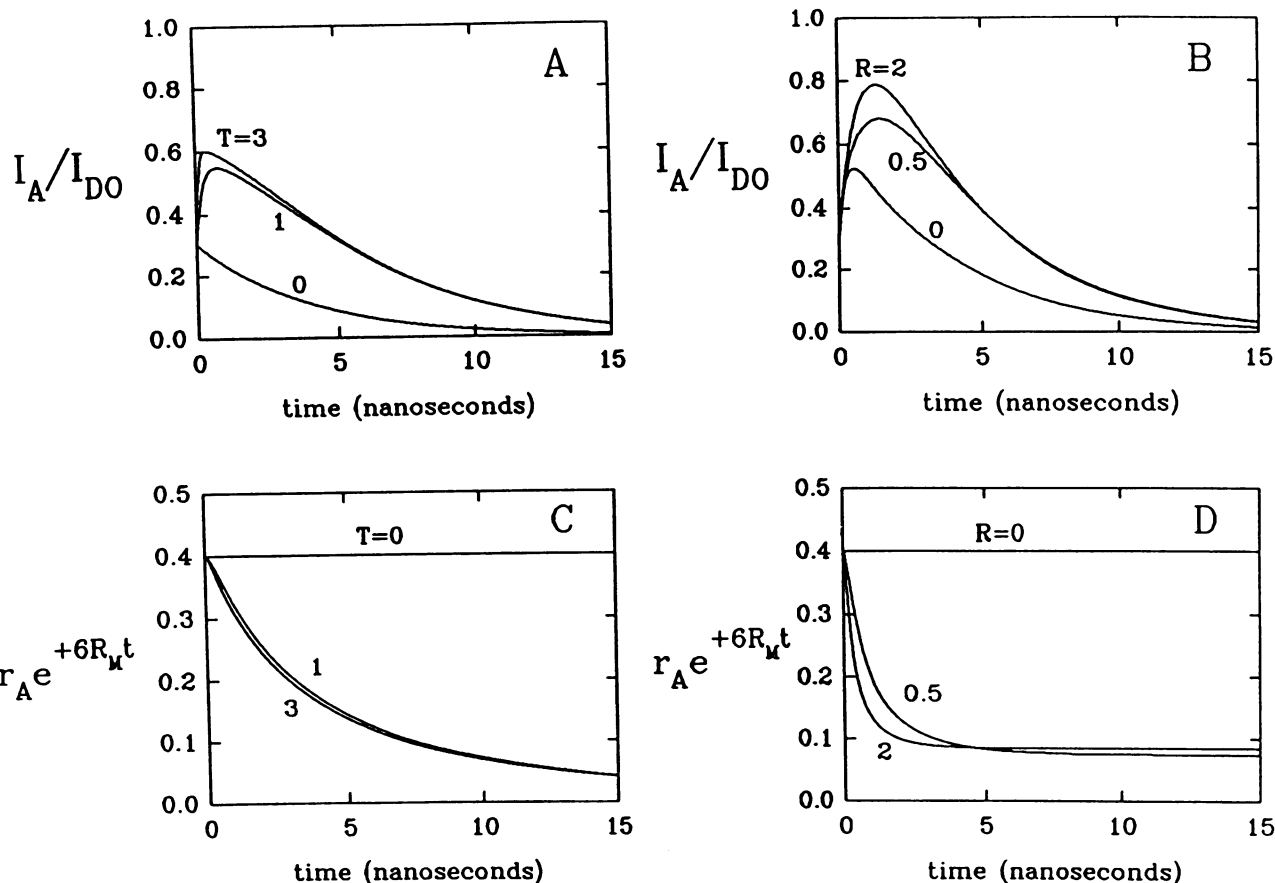
FIGURE 9   Rotational motion only in an isotropic system. The dependence of the time-resolved acceptor fluorescence and anisotropy on the rate of transfer and rotation is shown for example 2. T is the rate of transfer from the donor to the acceptor at unit orientation factor, k_D^{-1} = 6 ns (k_D is the rate of radiative decay of the donor), k_A^{-1} = 4 ns (k_A is the rate of radiative decay of the acceptor), and $\epsilon = I_{A0}/I_{D0}$ = 0.3 (ϵ is the ratio of acceptor absorbance over donor absorbance at donor excitation wavelengths). Here R and R_M represent rotational rate constants. Compare with Fig. 10, where R and R_M denote rotational diffusion constants, and the size of the cutoff matrices is 11×11 (see Appendix D). (A) Intensity; (C) anisotropy with R = 0.1 ns^{-1}, T = 0, 1, and 3 ns^{-1}. (B) Intensity; (D) anisotropy with R = 0, 0.5, and 2 ns^{-1}, T = 1 ns^{-1}. The anisotropy does not depend on R_M except for a factor $\exp(-6R_M t)$. The anisotropy divided by this factor is plotted in Figs. 9, C and D and 10, C and D.

values with coefficients adjusted to match the time 0 values (Appendix E). An example of a solution is shown for a number of time slices in Figure 12, with and without translational motion. The donor intensity is given by $I_D(t) = I_{D0} \sum_{m=1}^{N} x_m$. The dependence on the rate of translation and the rate of transfer is illustrated in Figure 13 below.

(g) The intensity of the acceptor fluorescence is $I_A(t) = I_{D0} \sum_{m=1}^{N} y_m$.

(h) The equation for $y_m(t)$ reads (see Appendix E) in the case N = 4:

$$\frac{d}{dt}\begin{pmatrix} y_1 \\ y_2 \\ y_3 \\ y_4 \end{pmatrix} = \begin{pmatrix} D_1 & Je^{-P_1} & 0 & 0 \\ Je^{-P_2} & D_2 & Je^{-P_2} & 0 \\ 0 & Je^{-P_3} & D_3 & Je^{-P_3} \\ 0 & 0 & Je^{-P_4} & D_4 \end{pmatrix}\begin{pmatrix} y_1 \\ y_2 \\ y_3 \\ y_4 \end{pmatrix}$$
$$+ \begin{pmatrix} T_1 x_1 \\ T_2 x_2 \\ T_3 x_3 \\ T_4 x_4 \end{pmatrix}$$

$$D_1 = -k_A - Je^{-P_2}$$
$$D_2 = -k_A - J(e^{-P_1} + e^{-P_3})$$
$$D_3 = -k_A - J(e^{-P_2} + e^{-P_4})$$
$$D_4 = -k_A - Je^{-P_3}, \tag{17}$$

where k_A is the rate of radiative acceptor decay. The general matrix equation for the y values at any value of N and its solution is given in Appendix E. Since the acceptor intensity is proportional to the sum of all the y components, an equation for the acceptor intensity can be obtained from the matrix equation for the acceptor by summing over the rows. This equation reads:

$$\frac{d}{dt} I_A = -k_A I_A + I_{D0} \sum_{m=1}^{N} T_m x_m. \tag{18}$$

Immediately after the flash I_A equals ϵI_{D0}, where ϵ is the ratio of the direct acceptor fluorescence over the donor fluorescence at the wavelength where the donor is
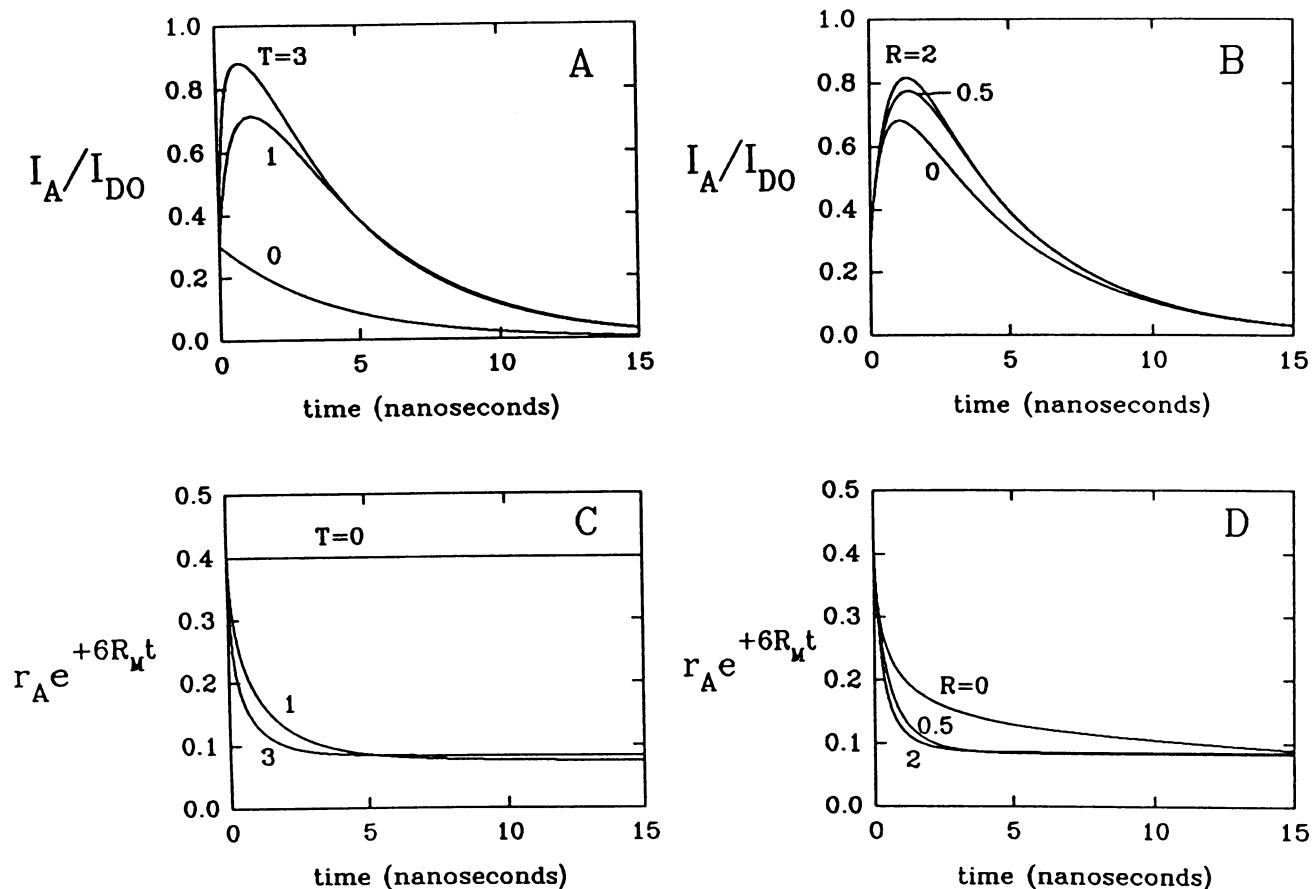
FIGURE 10 Profile of an isotropic system, per Fig. 9, with these exceptions: here R and R_M denote rotational diffusion constants. Here the size of the cutoff matrices is 11×11 (see Appendix D).
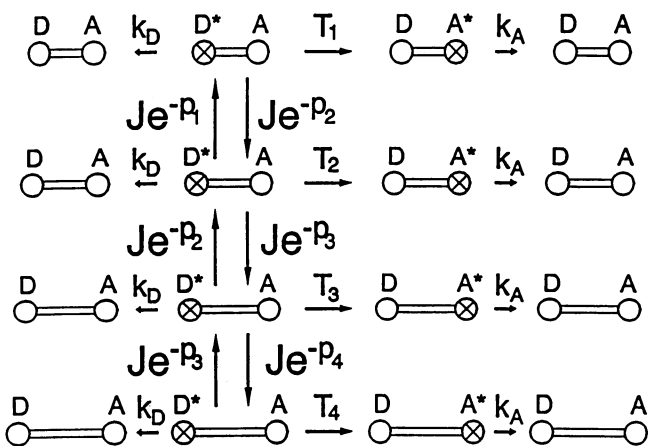

FIGURE 11 Translational motion only. The states and transitions for example 3 are shown in the case of four donor states. Dumbbells represent states for linear molecules with a donor on one end and an acceptor on the other end. States with an excited donor (D^*, A), with an excited acceptor (D, A^*), and without excitation (D, A) are shown. T_i ($i = 1, 2, 3, 4$) is the rate of transfer in state 1, 2, 3, or 4, k_D is the rate of radiative decay of the donor, k_A is the rate of radiative decay of the acceptor, and J is the rate of intermolecular translation. The origin of the exponential factors e^{-p_i} ($i = 1, 2, 3, 4$) is explained in the text.

excited. The solution of this equation with this boundary condition is:

$$I_A = I_{DO}\left[\epsilon e^{-k_A t} + \sum_{m=1}^{N} \sum_{l=1}^{N} T_m C(m, l) \frac{e^{-\lambda_l t} - e^{k_A t}}{k_A - \lambda_l} \right], \quad (19)$$

where $C(m, l)$ is the mth component of eigenvector l with eigenvalue λ_l of the matrix for the fractions x_m (m = $1 \cdots N$) matching the boundary condition (see Appendix E). The dependence of I_A on the rate of transfer and translation is illustrated in Figure 14, below.

DISCUSSION

In our treatment of FET we have adopted the standard assumption that the light levels used for excitation are low enough that the probability of an excited donor and an excited acceptor being in the same molecule or being close to each other is essentially zero. Although this is the usual experimental situation, it should be noted that it is not the only possibility, as pulsed laser excitation can provide near-saturation light levels.

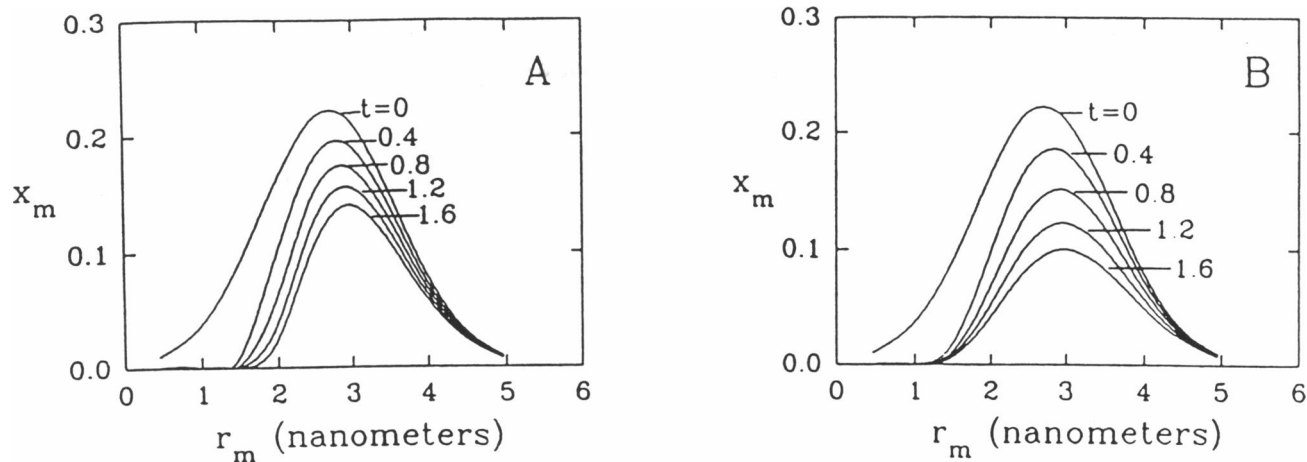The effect of FET on the distribution of excited donors is very sensitive to motion. The interdependence is

FIGURE 12 Translational motion only. Decrease in the fraction of excited molecules for example 3 in a state versus the donor–acceptor distance in that state starting at $t = 0$ (the time of the flash excitation) with subsequent time slices every 0.4 ns, R_0 = the Förster distance = 2.7 nm, k_D = the inverse of the donor radiative decay rate = $^1/_6$ ns^{-1}, s = the shortest donor–acceptor distance (occurring in state 1) = 1 nm, a = the medium donor–acceptor distance = 3 nm, σ = the width of the Gaussian distribution = 0.5 nm, N = the number of states = 10. (A) D_L = the lateral diffusion constant (defined in the text) = 0; (B) D_L = 0.2 nm^2/ns. A spline is fitted through the points.

nicely demonstrated in the extension of the first example to a system with infinite number of states. In that case, the first example becomes equivalent to a donor undergoing rotational diffusion, whereas transfer occurs to an acceptor that is fixed along the z-axis (see Appendix B). Consider in this situation the evolution in time of a polar plot of the distribution function, W_D, of excited donors, which is represented by a surface around the origin such that the distance between the origin and the surface along a line making an angle θ with the z-axis is proportional to the number of donors that are excited with their transition moment along that direction. Figure 15 shows the polar plots of W_D and illustrates the shape changes occurring when the system evolves from the time 0 $W_D = \cos^2 \theta$ to a "peanut" and eventually to a sphere

(not shown) in the case of rotational diffusion only, toward a "bowl-on-a-mirror" in the case of transfer only, and toward a "donut" if both transfer and diffusion processes are active. Figure 15 also helps to understand some surprising features of our results. One of these features is that in example 1 the anisotropy decays to negative values rather than to zero. The evolution of the distribution function toward a donut for the case of transfer in combination with rotation explains this behavior. In example 2, however, where there is transfer to a randomly oriented acceptor population from a freely rotating donor population, the anisotropy decays to positive values in the limit $R_M = 0$. This response can be understood when one realizes that about a third of the donor population (the ones that have the acceptor more or less
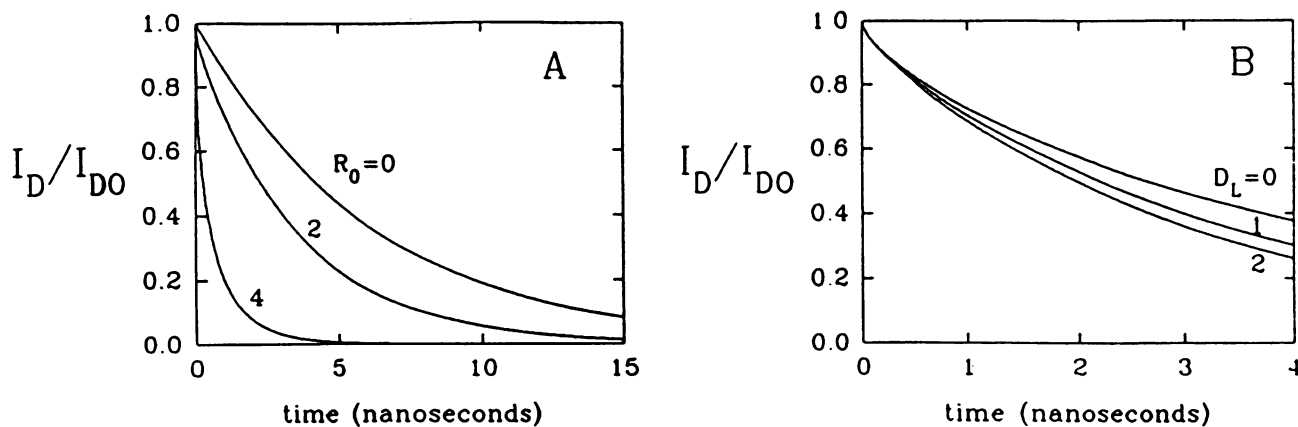

FIGURE 13 Translational motion only. The donor intensity over the initial donor intensity versus the time after the flash in example 3, for N = the number of states = 10, k_D = the inverse of the donor radiative decay rate = $^1/_6$ ns^{-1}, s = the shortest donor–acceptor distance (occurring in state 1) = 1 nm, a = the medium donor–acceptor distance = 3 nm, σ = the width of the Gaussian distribution = 0.5 nm. (A) D_L = the lateral diffusion constant (defined in the text) = 1 nm^2/ns, R_0 = the Förster distance = 0, 2, 4 nm; (B) R_0 = 2 nm, D_L = 0, 1, 2 nm^2/ns.
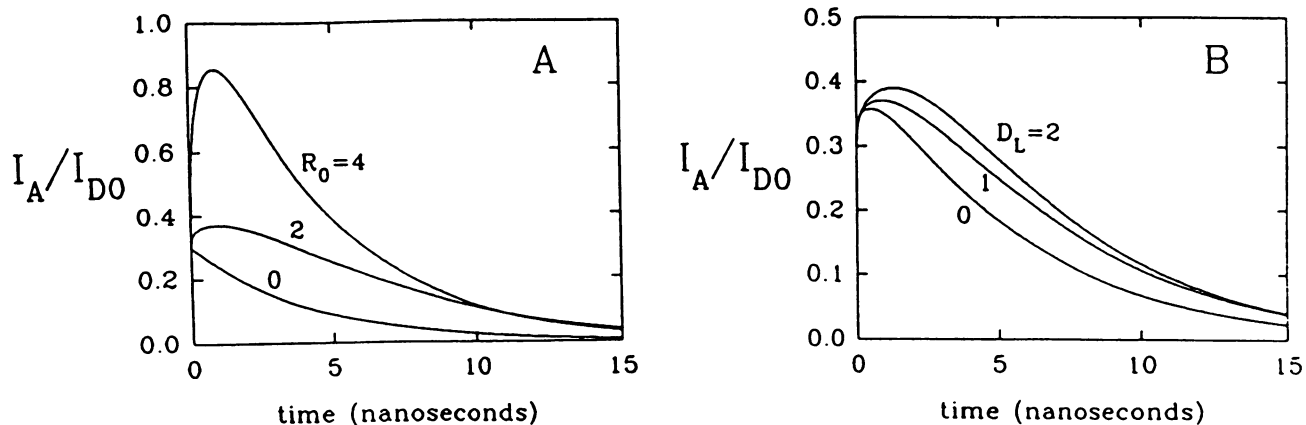
FIGURE 14 Translational motion only. The acceptor intensity over the initial donor intensity versus the time after the flash in example 3, for N = the number of states = 10, k_D = the inverse of the donor radiative decay rate = $^1/_6$ ns^{-1}, s = the shortest donor–acceptor distance (occurring in state 1) = 1 nm, a = the medium donor–acceptor distance = 3 nm, σ = the width of the Gaussian distribution = 0.5 nm, $\epsilon = I_{A0}/I_{D0}$ has been set equal to 0.3 (ϵ is the ratio of acceptor absorbance over donor absorbance at donor excitation wavelengths). (A) D_L = the lateral diffusion constant (defined in the text) = 1 nm^2/ns, R_0 = the Förster distance = 0, 2, 4 nm; (B) R_0 = 2 nm, D_L = 0, 1, 2 nm^2/ns.

aligned with the z-axis) behave as in example 1 but the others have a distribution that will decay toward deformed peanuts, and these will go slower. Another peculiarity is that in the intensity decay of the first example there is a crossover point, where at times before this point increasing the rate of rotation slows down the decay, whereas at later times increasing this rate speeds up the decay. To understand this characteristic, note that the distribution in Figure 15 acquires a "dip" at zero
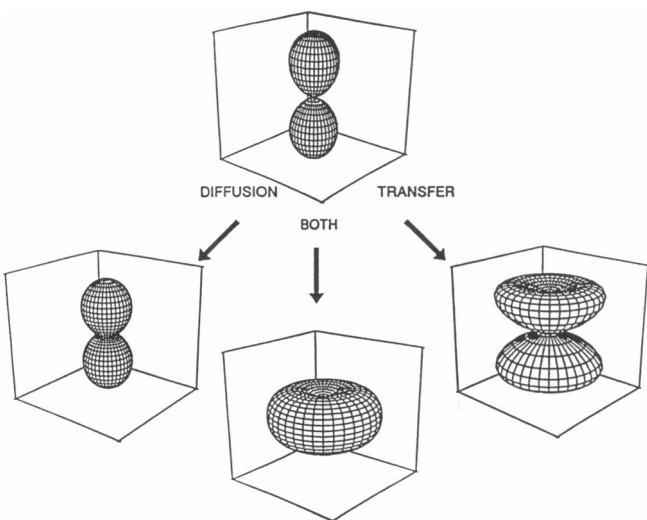

FIGURE 15 Polar plots for the distribution function W_D in which the distance from the center to the surface along a line at an angle θ from the vertical represents the value for W_D at that angle. The polar plot at the top corresponds to t = 0, W_D = cos^2 θ, and has boxside = 2; the one on the left is for t = 0.1 ns, R = 1 ns^{-1}, k_D = T = 0 with boxside = 1.6; the plot on the right refers to t = 0.1 ns, k_D = R = 0 ns^{-1}, T = 24 ns^{-1} with boxside = 0.3; the one at the bottom is for t = 0.1 ns, R = 1 ns^{-1}, k_D = 0, T = 40 ns^{-1} with boxside = 0.2.

degrees after a while. The crossover point probably corresponds with the time where this dip is substantial, so that before this point more rotation means a more spherical distribution with a lower top (from where there is a lot of transfer) with less decay, and after the crossover point more rotation would help to fill up the dip yielding a stronger decay. The location of the crossover point shifts if the motional step changes in size. Therefore, the T = 1 curve for R = 0.1 is intermediate between those for R = 0 and R = 0.5 in Figure 3, A and B (large motional step), whereas this is not the case for the curves shown in Figure 4, A and B (small motional step).

The main contribution of this article is that it provides a general method of taking into account the effects of motion when fluorescence energy transfer occurs. A secondary result of this work is that the time-resolved fluorescence is sensitive to the size of the motional step if FET occurs. That is, this study indicates that time-resolved energy transfer measurements in proteins (or in other systems) should be capable of determining whether localized motion of individual residues (or, more generally, of individual components of the system) more closely follows classical diffusion or discrete transitions between a relatively small number of states. Comparing the results of example 1 with those of the diffusion equation for that case (Appendix B) shows that if there is no transfer, then there is no difference between diffusion and 90° rotational jumps. On the other hand, if the rate of transfer is nonzero, then there is a marked difference, as the comparison of Figures 3 and 4 suggests. In example 1, the initial slope of the donor fluorescence anisotropy, $(d/dt)r_D(0)$, is equal to $-(72/175)T - (12/5)R$ in the case of diffusion but is equal to $-(252/175)T - (12/5)R$ in the case of 90° jumps. Furthermore, the donor anisotropy at times much larger than the fluorescence lifetime, $r_{D\infty}$, is equal to -0.1325 for $T = 2R$ in the
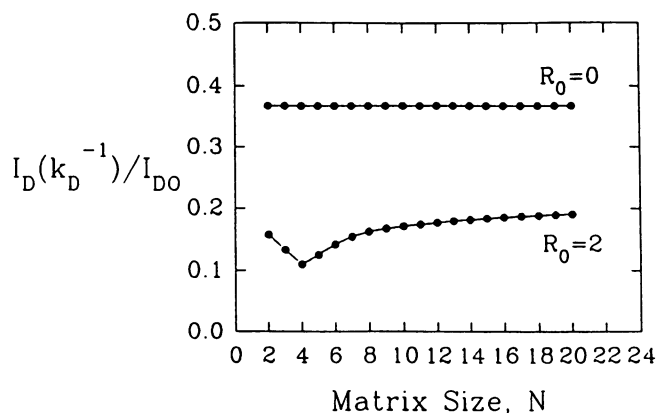
FIGURE 16 The effect of the size of the motional step that decreases as N, the number of states, increases for the third example (translational motion only). The donor intensity at $t = 1/k_D$ is plotted versus N, in the absence of transfer (R_0 = the Förster distance = 0) and in the case that there is transfer (R_0 = 2 nm) with D_L = 1 nm^2/ns, a = 3 nm, σ = 1 nm, s = 0.5 nm, and k_D = $^1/_6$ ns^{-1}.

case of diffusion but is equal to -0.2646 for $T = 2R$ in the case of 90° jumps. Differences between diffusion and 90° jumps occur also in the second example only if there is transfer (compare Figure 7 with Figure 8 and Figure 9 with Figure 10). Dramatic differences appear in the acceptor anisotropy; e.g., $r_A(0)$ in the case of $\epsilon = 0$ is equal to 0.4 for 90° jumps but is equal to 0.16 for diffusion, and $(d/dt)r_A(0)$ equals $-(12/5)R_M$ independent of ϵ for 90° jumps but equals $-(12/5)R_M - (8T/25\epsilon)$ for diffusion. In example 3, the effect of the size of the motional step (the effect of N = matrix size) is shown in Figure 16. Note that in the absence of transfer the intensity is independent of the number of states and, therefore, independent of the size of the motional step. If transfer occurs, however, the intensity for large translational jumps (N = 20) is 1.8 times the intensity for $N = 4$.

We have given up trying to derive general formulas for the fluorescence intensity and anisotropy for moving donors and acceptors. Instead, we have introduced a recipe for designing models applicable to specific cases based on the idea that the dynamics of a donor–acceptor system can be approximated by transitions between a finite number of states. It should be emphasized that this matrix methodology simple represents a foundation (not a final product) for the analysis of energy transfer in complex biological systems. For the analysis of energy transfer in proteins, for example, a variety of extensions to example 2 or 3 are required. The most crucial additions will be to allow the donor–acceptor separation vector to have any arbitrary angle and the initial acceptor dipole to have any angle with respect to the laboratory frame. In addition, a number of simplifying assumptions have been made, such as (a) the quantum yield is assumed to equal unity; (b) both donor and acceptor have single transition moments; (c) the molecules perform

either rotational or translational motion; and (d) equilibrium distributions of orientations are isotropic. Although most of these assumptions cannot be realized completely experimentally, our models approach some experimental situations where the observables calculated here could actually be measured and our recipe applied to gain useful insight into molecular motions. For example, our first model (this is actually the Berger–Vanderkooi model) would represent an oriented membrane with a protein embedded in it containing an acceptor with its transition moment along the membrane normal and a donor connected to the exterior of the protein where it would be allowed to rotate freely with very little translational freedom. The membrane would need to be oriented with its normal along the incoming polarization direction. Our second example represents such a macromolecule in solution, and the third example is very similar to a model discussed in the literature (references 5 and 13). The applicability of this model is discussed by Haas and co-workers (5, 13). These three cases approximate the restriction of motion that is effectively either rotation or translation. Our recipe is applicable to experimental situations in which both types of motion occur. Note also that the assumption of a quantum yield of unity does not present a real problem if k_D would be redefined as the sum of all radiative and nonradiative decay constants that are orientation or position independent.

An advantage of matrix methods and eigenvalue–eigenvector calculations is that they are numerically extremely fast. The diffusion model in Appendix B is one of the cases introduced by Berger and Vanderkooi (6), who solved it by Brownian dynamics calculations. Our method of finding the intensity and anisotropy using eigenvalues and eigenvectors (see Appendix B) is ∼120 times faster than their Brownian dynamics method. For the analysis of energy transfer in small flexible peptides, the model in example 3 can be immediately utilized. The solutions obtained for that example were similar to that obtained by Beechem and Haas (5); however, the methodology described in the present article can determine these solutions much faster. The obvious extension of this method for peptides will be to add different orientational states and rotational transitions between the states. Information on donor and acceptor fluorescence intensities could be combined with donor and acceptor fluorescence anisotropies (in the absence and presence of transfer). This work is underway.

The photoselection criterium used in examples 1 and 2 should be improved. It would be better to introduce a local coordinate system at random Euler angles with respect to the laboratory (x, y, z) system. The probabilities that the states are occupied and their time 0 values will then depend on these Euler angles. The intensities and anisotropies can be calculated by expressing them in these (time-dependent) probabilities and averaging over the Euler angles (16).

Our approach can be considered as an extension of the work by Piston and Gratton (11) and Weber (12) for fluorescence depolarization to the field of FET and polarized FET. Our work is also related to recent theoretical contributions by Szabo and co-workers (17, and references therein) and by Cross et al. (18).

APPENDIX A

This appendix contains the details of the mathematics for example 1 and follows the eight steps in the recipe for model design.

(a) Instead of the three states, x_D, y_D, and z_D, one could define six states for the excited donor:

x_P = state in which the donor moment is along the positive x-axis,

x_P = the probability that x_P is occupied,

x_N = state in which the donor moment is along the negative x-axis,

x_N = the probability that x_N is occupied,

y_P = state in which the donor moment is along the positive y-axis,

y_P = the probability that y_P is occupied,

y_N = state in which the donor moment is along the negative y-axis,

y_N = the probability that y_N is occupied,

z_P = state in which the donor moment is along the positive z-axis,

z_P = the probability that z_P is occupied,

z_N = state in which the donor moment is along the negative z-axis,

z_N = the probability that z_N is occupied.

The excited donor can lose energy by radiative decay at a rate k_D or by FET at a rate $T \times OF$, where OF is the orientation factor, kappa-squared that is defined as:

$$OF = (\cos \alpha - 3 \cos \beta \cos \gamma)^2, \quad (A1)$$

where α denotes the angle between donor and acceptor transition moments, β stands for the angle between donor moment and donor–acceptor separation vector, and γ is the angle between acceptor moment and this vector (7). In example 1, the acceptor moment is permanently aligned with the z-axis. Consequently, OF equals 4 in z_P and z_N and vanishes in the other states. The rotational motion is modeled by allowing 90° jumps at a rate R. That is, transitions at a rate R occur from x_P

or x_N to y_P, y_N, z_P, or z_N, from y_P or y_N to x_P, x_N, z_P, or z_N, and from z_P or z_N to x_P, x_N, y_P, or y_N. Consequently, the matrix equation for x_P, x_N, y_P, y_N, z_P, and z_N reads:

$$\frac{d}{dt}\begin{pmatrix} x_P \\ x_N \\ y_P \\ y_N \\ z_P \\ z_N \end{pmatrix} = \begin{pmatrix} -a_1 & 0 & R & R & R & R \\ 0 & -a_1 & R & R & R & R \\ R & R & -a_1 & 0 & R & R \\ R & R & 0 & -a_1 & R & R \\ R & R & R & R & -a_2 & 0 \\ R & R & R & R & 0 & -a_2 \end{pmatrix}\begin{pmatrix} x_P \\ x_N \\ y_P \\ y_N \\ z_P \\ z_N \end{pmatrix}, \quad (A2)$$

where a_1 and a_2 are defined in Eq. (1) and t denotes the time after the flash. It is convenient to apply the transformation of (A3), below.

$$\begin{cases} x_D = x_P + x_N & x_M = x_P - x_N \\ y_D = y_P + y_N & y_M = y_P - y_N \\ z_D = z_P + z_N & z_M = z_P - z_N. \end{cases} \quad (A3)$$

Adding the first and second, third and fourth, fifth and sixth rows in Eq. A2 and eliminating x_P, x_N, y_P, y_N, z_P, and z_N, using Eq. A3 yields Eq. 1. This procedure explains the factor 2 in $2R$ of Eq. 1. Subtracting the second from the first, the fourth from the third, the sixth from the fifth row and eliminating x_P, x_N, y_P, y_N, z_P, and z_N using Eq. A3 yields a diagonal matrix equation for x_M, y_M, and z_M with solution $x_M = y_M = z_M = 0$, because the initial values of these variables equal zero. As a result, the model of example 1 can conveniently be redefined as done in Figure 2 yielding the matrix equation of Eq. 1.

For steps b, c, d, and e, see the text above.

(f) Eq. 1 can be further simplified by the transformation,

$$\begin{cases} f_D = \frac{1}{2}(x_D - y_D) \\ h_D = \frac{1}{2}(x_D + y_D). \end{cases} \quad (A4)$$

Subtracting the second row from the first in Eq. 1 yields a linear differential equation in f_D, of which the solution is $f_D = 0$, because the initial values for x_D and y_D are equal to each other. Consequently, x_D and y_D are equal to each other at all times, and h_D equals x_D for all t. Adding the first two rows of Eq. 1 and eliminating x_D and y_D using Eq. A4 leads to:

$$\frac{d}{dt}\begin{pmatrix} h_D \\ z_D \end{pmatrix} = \begin{pmatrix} -k_D - 2R & 2R \\ 4R & -k_D - 4R - 4T \end{pmatrix}\begin{pmatrix} h_D \\ z_D \end{pmatrix}, \quad (A5)$$

with boundary condition, $h_D = x_D = 0.2$ and $z_D = 0.6$ for $t = 0$. The eigenvalues and eigenvectors of the matrix in Eq. A5 are:

EIGENVALUES $\qquad \lambda_1 = -k_D - 3R - 2T + W \qquad \lambda_2 = -k_D - 3R - 2T - W$

corresponding EIGENVECTORS $\qquad \begin{pmatrix} 2R \\ -R - 2T + W \end{pmatrix} \qquad \begin{pmatrix} 2R \\ -R - 2T - W \end{pmatrix}.$

Here, W is as defined in Eq. 2b. The solution of Eq. A5 can be written in terms of these eigenvalues and eigenvectors as:

$$\begin{pmatrix} h_D \\ z_D \end{pmatrix} = c_1 \begin{pmatrix} 2R \\ -R - 2T + W \end{pmatrix} e^{-(k_D + 3R + 2T - W)t}$$

$$+ c_2 \begin{pmatrix} 2R \\ -R - 2T - W \end{pmatrix} e^{-(k_D + 3R + 2T + W)t}, \quad (A6)$$

where the coefficients c_1 and c_2 are to be chosen such that $h_D = x_D = 0.2$ and $z_D = 0.6$ for $t = 0$. From this condition we obtain:

$$c_1 = [W + 7R + 2T]/(20RW),$$
$$c_2 = [W - 7R - 2T]/(20RW). \quad (A7)$$

Substituting Eq. A7 into Eq. A6 yields:

$$h_D = x_D = \frac{0.1}{W} e^{-(k_D + 3R + 2T - W)t}$$

$$\times \{ W + 7R + 2T + (W - 7R - 2T)e^{-2Wt} \} \quad (A8a)$$

$$z_D = \frac{0.1}{W} e^{-(k_D+3R+2T-W)t}$$

$$\times \{3W + R - 6T + (3W - R + 6T)e^{-2Wt}\}. \quad (A8b)$$

Substituting Eq. A8 into $I_D = I_{D0}(z_D + 2x_D)$ and $r_D = (z_D - x_D)/(z_D + 2x_D)$ produces Eq. 2.

(g) See text.

(h) Because both x_A and y_A equal 0 at time 0 and are not coupled to z_D, it follows from Eq. 3 that x_A and y_A equal 0 at all times. The solution for the differential equation for z_A in Eq. 3 with $z_A(0) = \epsilon$ (see 4) has the form: $z_A = e^{-k_A t}G$, yielding the following equation for G:

$$\frac{d}{dt} G = 4Tz_D e^{k_A t} = \frac{0.4T}{W}(3W + R - 6T)e^{(k_A-k_D-3R-2T+w)t}$$

$$+ \frac{0.4T}{W}(3W - R + 6T)e^{k_A-k_D-3R-2T-w)t}, \quad (A9)$$

with $G(0) = \epsilon$. The solution of Eq. A9 with this time 0 condition is $G = \epsilon + e^{k_A t}(A_A + B_A)$, where A_A and B_A are given in Eqs. 4b and 4c, respectively. It follows that z_A is given by $z_A = \epsilon e^{-k_A t} + A_A + B_A$.

APPENDIX B

The three-state model of example 1 can be generalized by dividing the range of 2π for the azimuthal angle φ of the donor transition moment in equal parts of $\Delta\varphi$ and the range of π for the polar angle θ in equal divisions of $\Delta\theta$ and by introducing a distribution function $W_D(\theta, \varphi)$ so that $W_D(\theta, \varphi)\Delta\theta \sin \theta \Delta\varphi$ represents the number of molecules with a polar angle between θ and $\theta + \Delta\theta$ and an azimuthal angle between φ and $\varphi + \Delta\varphi$. The generalized matrix equation now becomes:

$$\frac{\partial}{\partial t} W_D(\theta, \varphi) \sin \theta \Delta\theta\Delta\varphi$$

$$= J_V W_D(\theta - \Delta\theta, \varphi)\left[\sin \theta - \frac{1}{2} \Delta\theta \cos \theta\right]\Delta\theta\Delta\varphi$$

$$+ J_V W_D(\theta + \Delta\theta, \varphi)\left[\sin \theta + \frac{1}{2} \Delta\theta \cos \theta\right]\Delta\theta\Delta\varphi$$

$$+ J_H W_D(\theta, \varphi + \Delta\varphi) \sin \theta\Delta\theta\Delta\varphi$$

$$+ J_H W_D(\theta, \varphi - \Delta\varphi) \sin \theta\Delta\theta\Delta\varphi$$

$$- (2J_V + 2J_H + k_D + 4T \cos^2 \theta)W_D(\theta, \varphi) \sin \theta\Delta\theta\Delta\varphi, \quad (B1)$$

where J_V and J_H are rate constants, $[\sin \theta - \frac{1}{2} \Delta\theta \cos \theta]\Delta\theta\Delta\varphi$ is the infinitesimal solid angle around $(\theta - \Delta\theta, \varphi)$, and $[\sin \theta + \frac{1}{2}\Delta\theta \cos \theta]\Delta\theta\Delta\varphi$ is the infinitesimal solid angle around $(\theta + \Delta\theta, \varphi)$. Using:

$$(1) \quad \frac{1}{2} [W_D(\theta + \Delta\theta, \phi) - W_D(\theta - \Delta\theta, \phi)]$$

$$= \Delta\theta \frac{\partial}{\partial\theta} W_D(\theta, \phi), \quad (B2a)$$

$$(2) \quad W_D(\theta + \Delta\theta, \phi) - W_D(\theta, \phi)$$

$$= \Delta\theta \frac{\partial}{\partial\theta} W_D\left(\theta + \frac{1}{2} \Delta\theta, \phi\right), \quad (B2b)$$

$$(3) \quad W_D(\theta - \Delta\theta, \phi) - W_D(\theta, \phi)$$

$$= -\Delta\theta \frac{\partial}{\partial\theta} W_D\left(\theta - \frac{1}{2} \Delta\theta, \phi\right), \quad (B2c)$$

$$(4) \quad W_D(\theta, \phi + \Delta\varphi) - W_D(\theta, \phi)$$

$$= \Delta\varphi \frac{\partial}{\partial\varphi} W_D\left(\theta, \phi + \frac{1}{2} \Delta\varphi\right), \quad (B2d)$$

$$(5) \quad W_D(\theta, \phi - \Delta\varphi) - W_D(\theta, \phi)$$

$$= -\Delta\varphi \frac{\partial}{\partial\varphi} W_D\left(\theta, \phi - \frac{1}{2} \Delta\varphi\right), \quad (B2e)$$

$$(6) \quad \frac{\partial}{\partial\theta} W_D\left(\theta + \frac{1}{2} \Delta\theta, \phi\right) - \frac{\partial}{\partial\theta} W_D\left(\theta - \frac{1}{2} \Delta\theta, \phi\right)$$

$$= \Delta\theta \frac{\partial^2}{\partial\theta^2} W_D(\theta, \phi), \quad (B2f)$$

$$(7) \quad \frac{\partial}{\partial\varphi} W_D\left(\theta, \phi + \frac{1}{2} \Delta\varphi\right) - \frac{\partial}{\partial\varphi} W_D\left(\theta, \phi - \frac{1}{2} \Delta\varphi\right)$$

$$= \Delta\varphi \frac{\partial^2}{\partial\varphi^2} W_D(\theta, \phi), \quad (B2g)$$

Eq. B1 can be rewritten as:

$$\frac{\partial}{\partial t} W_D(\theta, \varphi)$$

$$= J_V(\Delta\theta)^2\left\{\frac{\partial^2}{\partial\theta^2} W_D(\theta, \varphi) + \frac{\cos \theta}{\sin \theta} \frac{\partial}{\partial\theta} W_D(\theta, \varphi)\right\}$$

$$+ J_H(\Delta\varphi)^2 \frac{\partial^2}{\partial\varphi^2} W_D(\theta, \varphi)$$

$$- (k_D + 4T \cos^2 \theta)W_D(\theta, \varphi). \quad (B3)$$

If we choose $\Delta\varphi \sin \theta = \Delta\theta$, then the solid angle sectors become square, so that J_V and J_H must be equal to each other. With the definition $J_V(\Delta\theta)^2 = J_H(\sin \theta\Delta\varphi)^2 = R$, Eq. B3 reduces to:

$$\frac{\partial}{\partial t} W_D = -k_D W_D + R\nabla_1^2 W_D - 4T(\cos^2 \theta)W_D, \quad (B4)$$

where ∇_1^2 denotes the angular part of the Laplacian:

$$\nabla_1^2 W_D = \frac{\partial^2}{\partial\theta^2} W_D + \frac{\cos \theta}{\sin \theta} \frac{\partial}{\partial\theta} W_D + \frac{1}{\sin^2 \varphi} \frac{\partial^2}{\partial\varphi^2} W_D. \quad (B5)$$

The distribution function $W_D = W_D(\theta, \varphi)$ can be expanded in the even Legendre polynomials of $\cos \theta$, as follows,

$$W_D = \sum_{n=1}^{\infty} V_n(t)P_{2n-2}(\cos \theta), \quad (B6)$$

where the coefficients V_1, V_2, V_3, etc. are functions of the time t. Eq. B4 can be transformed into a set of linear equations in the coefficients V_n ($n = 1 \cdots \infty$) by applying the following properties of Legendre polynomials (Eqs. B7 [from reference 19] and B8):

$$\nabla_1^2 P_{2n-2}(\cos \theta) = -(2n - 2)(2n - 1)P_{2n-2}(\cos \theta)$$

$$(n = 1, 2, \cdots) \quad (B7)$$

$$(\cos \theta)^2 P_k^m(\cos \theta)$$

$$= \frac{(k + 2 - m)(k + 1 - m)}{(2k + 3)(2k + 1)} P_{k+2}^m(\cos \theta)$$

$$+ \frac{(2k^2 + 2k - 1 - 2m^2)}{(2k + 3)(2k - 1)} P_k^m(\cos \theta)$$

$$+ \frac{(k + m)(k - 1 + m)}{(2k + 1)(2k - 1)} P_{k-2}^m(\cos \theta), \quad (B8)$$

where m and k are integers. Here, m = 0 and $k = 2n - 2$. For m = 0, we define $P_k^m(\cos \theta) = P_k(\cos \theta)$; for m $\neq$ 0, $P_k^m(\cos \theta)$ denote associated Legendre functions, which will be used in Appendix D. Eq. B8 follows from repeated application of the relation $(2N + 1)xP_N^m(x) = (N + m)P_{N-1}^m(x) + (N - m + 1)P_{N+1}^m(x)\{N = 1 \cdots \infty\}$ (19). Application

of Eqs. B7 and B8, the orthogonality and the completeness of the Legendre polynomials, allows us to rewrite Eq. B4 as:

$$\frac{d}{dt} V_n(t) = \sum_{m=1}^{\infty} M(n, m) V_m(t) \quad (n = 1 \cdots \infty), \quad (B9a)$$

where n and m are integers and all matrix elements $M(n, m)$ vanish except the ones on the diagonal, subdiagonal, and superdiagonal, which are, for $n = 1, 2, \cdots \infty$:

$$M(n, n) = -k_D - (2n - 2)(2n - 1)R$$
$$- \frac{4(8n^2 - 12n + 3)T}{(4n - 5)(4n - 1)} \quad (B9b)$$

$$M(n, n + 1) = -\frac{8n(2n - 1)T}{(4n - 1)(4n + 1)} \quad (B9c)$$

$$M(n + 1, n) = -\frac{8n(2n - 1)T}{(4n - 1)(4n - 3)}. \quad (B9c)$$

Since at the time of the flash $t = 0$, $W_D = \cos^2 \theta = \frac{1}{3} + \frac{2}{3} P_2(\cos \theta)$, the time 0 values for the coefficients are $V_1(0) = \frac{1}{3}$, $V_2(0) = \frac{2}{3}$, and $V_n(0) = 0$ for $n > 2$. The intensity of the donor fluorescence response to an extremely short pulse is:

$$I_D(t) = \frac{3 I_{D0}}{4\pi} \int_0^{2\pi} \int_0^{\pi} W_D(\theta, \varphi) \sin \theta \, d\varphi \, d\theta$$
$$= 3 I_{D0} V_1(t), \quad (B10)$$

and the fluorescence anisotropy of the donor is:

$$r_D(t) = \frac{\int_0^{2\pi} \int_0^{\pi} P_2(\cos \theta) W_D(\theta, \varphi) \sin \theta \, d\varphi \, d\theta}{\int_0^{2\pi} \int_0^{\pi} W_D(\theta, \varphi) \sin \theta \, d\varphi \, d\theta}$$
$$= \frac{V_2(t)}{5 V_1(t)}. \quad (B11)$$

A series of approximations for these quantities can be calculated from the eigenvalues and eigenvectors of a series of truncated matrices, a 2 × 2, a 3 × 3, a 4 × 4 matrix, etc., that are truncated versions of the matrix in Eq. B9. That is, the $N \times N$ cutoff matrix or truncated version of the matrix in Eq. B9, $M_N(n, m)$, is defined as:

$$\begin{cases} M_N(n, m) = M(n, m) & \text{for} \quad n \le N \quad \text{and} \quad m \le N \\ M_N(n, m) = 0 & \text{for} \quad n > N \quad \text{and/or} \quad m > N. \end{cases}$$
$$(B12)$$

If $\lambda_m^{(N)}$ (m = $1 \cdots N$) denotes the mth eigenvalue of the matrix M_N and $E_N(n, m)$, the nth component of the corresponding eigenvector, numbered m, normalized such that $\sum_{m=1}^{N} E_N(1, m) = \frac{1}{3}$, $\sum_{m=1}^{N} E_N(2, m) = \frac{2}{3}$, and $\sum_{m=1}^{N} E_N(n, m) = 0$ for $2 < n \le N$, then the Nth order approximation to the solution of the coefficients V_n ($n = 1 \cdots N$) reads:

$$V_n = \sum_{m=1}^{N} E_N(n, m) \exp(\lambda_m^{(N)} t) \quad (n = 1 \cdots N). \quad (B13)$$

When I_D and r_D are calculated from Eqs. B10 and B11, respectively, using the approximations for V_1 and V_2 of Eq. B13 for N between 2 and 18, then for all choices of the parameters convergence is reached before $N = 6$. This behavior is illustrated in Figure 17. Therefore, the results shown in Figure 4 are calculated from 6 × 6 cutoff matrices. Note that for $T = 0$, i.e., in the absence of transfer, the matrix in Eq. B9 reduces to a diagonal matrix and the calculation of V_1 and V_2 becomes trivial, resulting in:

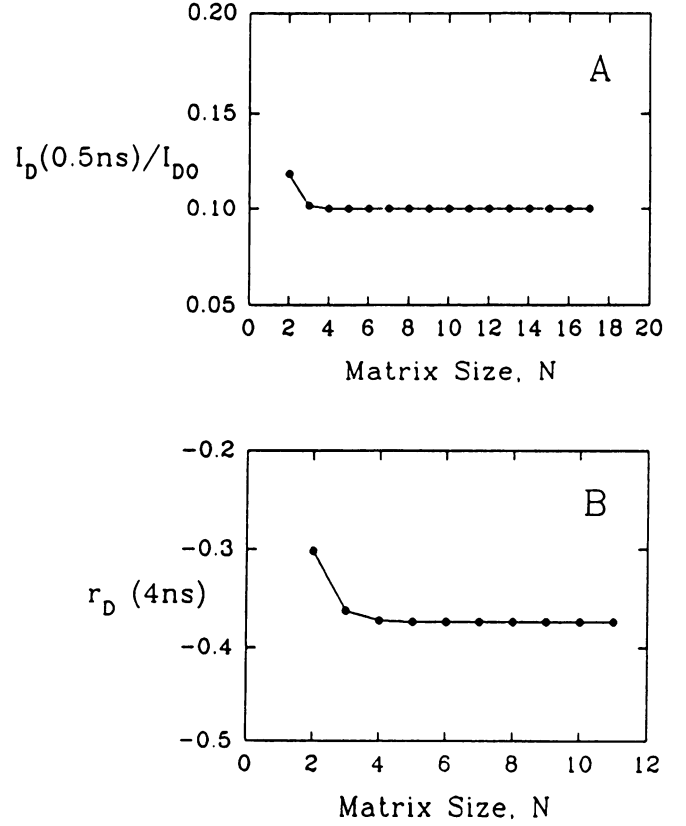$$I_D(t) = 3 I_{D0} V_1(t) = I_{D0} e^{-k_D t}, \quad (B14)$$

FIGURE 17   Results for I_D and r_D calculated for different cutoff matrices plotted versus the size N of $N \times N$ matrices ($1 < N < 18$). In both panels the following parameter values were used: $k_D = \frac{1}{6}$ ns^{-1}, $R = 0.1$ ns^{-1}, $T = 3$ ns^{-1}. (A) The donor intensity over its initial value at $t = 0.5$ ns is plotted versus N; (B) the donor anisotropy at $t = 4$ ns is shown. At these times the differences between initial and plateau values were essentially maximal.

and

$$r_D(t) = V_2(t)/(5 V_1(t))$$
$$= (\frac{2}{3} e^{-(k_D + 6R)t})/(5 \times \frac{1}{3} e^{-k_D t}) = \frac{2}{5} e^{-6Rt}. \quad (B15)$$

APPENDIX C

This appendix provides the derivations of the equations for example 2. The numbers below refer to the steps in the model design.

(a) The excited donor and acceptor states are defined in the text.

(b) The motional transitions are defined in Figures 5 and 6 and specified in Eq. 5, above. Again, the factors 2 in $2R$ and $2R_M$ are due to the fact that a 90° rotation is possible both from the positive and negative x, y, or z-axis. For steps c, d, and e see text.

(f) The eigenvalues and eigenvectors of the matrix in Eq. 5 can be derived by applying the transformation defined in Table 2.

Applying this transformation to Eq. 5 and rearranging terms leads to the following matrix equations:

$$\frac{d}{dt} \begin{pmatrix} a \\ b \end{pmatrix} = \begin{pmatrix} -k_D - 4R - 4T & 4R \\ 2R & -k_D - 2R \end{pmatrix} \begin{pmatrix} a \\ b \end{pmatrix} \quad (C1a)$$

$$dc/dt = -(k_D + 12 R_M + 6R)c \quad (C1b)$$

$$\frac{d}{dt} \begin{pmatrix} p \\ s \end{pmatrix} = \begin{pmatrix} -k_D - 4R - 4T - 6R_M & 4R \\ 2R & -k_D - 2R - 6R_M \end{pmatrix} \begin{pmatrix} p \\ s \end{pmatrix}$$
$$(C1c)$$

TABLE 2 Definition of *a*, *b*, *c*, *p*, *q*, *s*, *u*, *v*, and *w**

$a = \frac{1}{3}(x_1 + y_2 + z_3)$	$a_0 = \frac{1}{9}$	$x_1 = \frac{1}{3}(3a + 2p + 2q)$	$x_{10} = 1/15$
$b = \frac{1}{6}(y_1 + z_1 + x_2 + z_2 + x_3 + y_3)$	$b_0 = \frac{1}{9}$	$y_1 = \frac{1}{3}(3b + 3c + 2s + 2u + 2v + 2w)$	$y_{10} = 1/15$
$c = \frac{1}{6}(y_1 - z_1 + z_2 - x_2 + x_3 - y_3)$	$c_0 = 0$	$z_1 = \frac{1}{3}(3b - 3c + 2s + 2u - 2v - 2w)$	$z_{10} = \frac{1}{5}$
$p = \frac{1}{2}(x_1 - y_2)$	$p_0 = 0$	$x_2 = \frac{1}{3}(3b - 3c - 4s + 2u + 4v - 2w)$	$x_{20} = 1/15$
$q = \frac{1}{2}(x_1 - z_3)$	$q_0 = -1/15$	$y_2 = \frac{1}{3}(3a - 4p + 2q)$	$y_{20} = 1/15$
$s = \frac{1}{4}(y_1 + z_1 - x_2 - z_2)$	$s_0 = 0$	$z_2 = \frac{1}{3}(3b + 3c - 4s + 2u - 4v + 2w)$	$z_{20} = \frac{1}{5}$
$u = \frac{1}{4}(y_1 + z_1 - x_3 - y_3)$	$u_0 = 1/30$	$x_3 = \frac{1}{3}(3b + 3c + 2s - 4u + 2v - 4w)$	$x_{30} = 1/15$
$v = \frac{1}{4}(y_1 - z_1 - z_2 + x_2)$	$v_0 = -1/15$	$y_3 = \frac{1}{3}(3b - 3c + 2s - 4u - 2v + 4w)$	$y_{30} = 1/15$
$w = \frac{1}{4}(y_1 - z_1 - x_3 + y_3)$	$w_0 = -1/30$	$z_3 = \frac{1}{3}(3a + 2p - 4q)$	$z_{30} = \frac{1}{5}$

* Subscripts 0 indicate time 0 values.

$$dv/dt = -(k_D + 6R + 6R_M)v \qquad (C1d)$$

$$\frac{d}{dt}\begin{pmatrix} q \\ u \end{pmatrix} = \begin{pmatrix} -k_D - 4R - 6R_M - 4T & 4R \\ 2R & -k_D - 2R - 6R_M \end{pmatrix}\begin{pmatrix} q \\ u \end{pmatrix} \qquad (C1e)$$

$$dw/dt = -(k_D + 6R + 6R_M)w. \qquad (C1f)$$

Since the time 0 values (see Table 2) of c, p, and s are equal to zero, the solution of Eqs. C1b and C1c is $c = p = s = 0$. The solutions of Eqs. C1a, C1d, C1e, and C1f with the boundary conditions of Table 2 are obtained by methods similar to solving Eq. A5, above, and read:

$$a(t) = \frac{1}{18W}(W + 3R - 2T)\exp\{\lambda_1 t\}$$
$$+ \frac{1}{18W}(W - 3R - 2T)\exp\{\lambda_2 t\} \qquad (C2a)$$

$$b(t) = \frac{1}{18W}(W + 3R - 2T)\exp\{\lambda_1 t\}$$
$$+ \frac{1}{18W}(W - 3R - 2T)\exp\{\lambda_2 t\} \qquad (C2b)$$

$$v = -\frac{1}{15}e^{-(k_D + 6R + 6R_M)t} \qquad (C2c)$$

$$q(t) = \frac{1}{30W}(-W + 3R + 2T)\exp\{\mu_1 t\}$$
$$- \frac{1}{30W}(W + 3R + 2T)\exp\{\mu_2 t\} \qquad (C2e)$$

$$u(t) = \frac{1}{60W}(W - 3R + 2T)\exp\{\lambda_1 t\}$$
$$+ \frac{1}{60W}(W + 3R - 2T)\exp\{\lambda_2 t\} \qquad (C2f)$$

$$w = -\frac{1}{30}e^{-(k_D + 6R + 6R_M)t}, \qquad (C2g)$$

with $W = [8R^2 + (R + 2T)^2]^{0.5}$, $\lambda_1 = -k_D - 3R - 2T + W$, $\lambda_2 = -k_D - 3R - 2T - W$, $\mu_1 = \lambda_1 - 6R_M$, and $\mu_2 = \lambda_2 - 6R_M$. The intensity of the donor fluorescence is:

$$I_D = I_{D0}(z_1 + z_2 + z_3 + 2x_1 + 2x_2 + 2x_3)$$
$$= I_{D0}(3a + 6b + 2p - 2s + 2v - 4w) = I_{D0}(3a + 6b).$$

Substituting Eqs. C2a and C2b into this expression of the intensity yields Eq. 6a. For $T = 0$ (no transfer), Eq. 6a reduces to $I_D = I_{D0}\exp(-k_D t)$, as expected. The anisotropy of the donor fluorescence is:

$$r_D = \frac{z_1 + z_2 + z_3 - x_1 - x_2 - x_3}{z_1 + z_2 + z_3 + 2x_1 + 2x_2 + 2x_3}$$
$$= \frac{2u - 2q - 3v + 2w}{3a + 6b} = \frac{2u - 2q - 3v}{3a + 6b}.$$

Substituting Eqs. C2a–c, e, and f into this expression yields Eq. 6b. For $T = 0$ (no transfer), Eq. 6b reduces to $r_D = 0.4\exp\{-(6R + 6R_M)t\}$, as expected. Note that for $R = 0$, the anisotropy becomes $0.4\exp\{-6R_M t\}$, independent of the value of T.

(*g*) The acceptor fluorescence = $I_A = I_{D0}(z_A + 2x_A)$. The acceptor anisotropy = $r_A = (z_A - x_A)/(z_A + 2x_A)$.

(*h*) Adding the rows of Eq. 7 yields:

$$\frac{d}{dt}(x_A + y_A + z_A)$$
$$= -k_A(x_A + y_A + z_A) + 4T(x_1 + y_2 + z_3), \qquad (C3)$$

where $x_1 + y_2 + z_3 = 3a$ and the time 0 value for $x_A + y_A + z_A$ equals ϵ. The solution of Eq. C3 is:

$$x_A + y_A + z_A = \epsilon \times \exp\{-k_A t\}$$
$$+ \frac{2T(W + 3R - 2T)}{3W(k_A + \lambda_1)}[\exp\{\lambda_1 t\} - \exp\{-k_A t\}]$$
$$+ \frac{2T(W - 3R + 2T)}{3W(k_A + \lambda_2)}[\exp\{\lambda_2 t\} - \exp\{-k_A t\}]. \quad (C4)$$

Multiplying this expression with I_{D0} produces Eq. 8a. Subtracting the first row from the third row in Eq. 7 yields:

$$\frac{d}{dt}(z_A - x_A) = -(k_A + 6R_M)(z_A - x_A) + 4T(z_3 - x_1)$$
$$= -(k_A + 6R_M)(z_A - x_A) - 8Tq, \qquad (C5)$$

where the time 0 value for $z_A - x_A$ equals 0.4ϵ. The solution of Eq. C5 reads:

$$z_A - x_A = 0.4\epsilon \times \exp\{-(k_A + 6R_M)t\}$$
$$+ \frac{4T(W - 3R - 2T)}{15W(k_A + \mu_1 + 6R_M)}$$
$$\times [\exp\{\mu_1 t\} - \exp\{-(k_A + 6R_m)t\}]$$
$$+ \frac{4T(W + 3R - 2T)}{15W(k_A + \mu_2 + 6R_M)}$$
$$\times [\exp\{\mu_2 t\} - \exp\{-(k_A + 6R_M)t\}]. \qquad (C6)$$

Substituting Eqs. C4 and C6 into $r_A = (z_A - x_A)/(z_A + x_A + y_A) = (z_A - x_A)/(z_A + 2x_A)$ produces Eq. 8b.

APPENDIX D

The second example can be extended in the same way as the first, introducing more states and deriving a diffusion equation in terms of a distribution function $W_D = W_D(\theta_z, \theta, \varphi)$, where θ_z is the angle between the laboratory z-axis and the acceptor transition moment, θ is the angle

between the donor transition moment and the acceptor moment, and $\varphi = \varphi_D - \varphi_Z$. Here, φ_D is the angle between the projection of the donor moment on a plane perpendicular to the acceptor moment and the x'-axis, which is an arbitrary direction perpendicular to the acceptor moment, and φ_Z is the angle between the projection of the laboratory z-axis on a plane perpendicular to the acceptor moment and the x'-axis. Applying the same mathematical techniques as in deriving the diffusion Eq. B4 yields in this case:

$$\frac{\partial}{\partial t} W_D = -k_D W_D + R_M \nabla^2_{1M} W_D$$
$$+ R\nabla^2_1 W_D - 4T(\cos\theta)^2 W_D, \quad (D1)$$

where ∇^2_{1M} is the angular part of the Laplacian (as defined in Eq. B5) in terms of θ_Z and φ_Z and ∇^2_1 is that in terms of θ and φ_D. The time 0 value of W_D is $\cos^2\theta_D$, where θ_D is the angle between the laboratory z-axis and the donor transition moment. The addition theorem for Legendre polynomials allows for rewriting $\cos^2\theta_D$ as:

$$\cos^2\theta_D = {}^2/_3 P_2(\cos\theta_Z)P_2(\cos\theta)$$
$$+ {}^2/_9 P^1_2(\cos\theta_Z)P^1_2(\cos\theta)\cos\varphi$$
$$+ {}^1/_{18} P^2_2(\cos\theta_Z)P^2_2(\cos\theta)\cos 2\varphi$$
$$+ {}^1/_3 P_0(\cos\theta), \quad (D2)$$

where P^1_2 and P^2_2 denote associated Legendre functions and P_m (m = 0, 2) are Legendre polynomials ($P_0(z) = 1$, $P_2(z) = (3z^2 - 1)/2$). This form suggests that the following expansion of W_D in even Legendre polynomials and associated Legendre functions is useful:

$$W_D = \sum_{n=1}^{\infty} V_{n,0} P_2(\cos\theta_M)P_{2n-2}(\cos\theta)$$
$$+ \sum_{n=1}^{\infty} V_{n,1} P^1_2(\cos\theta_M)P^1_{2n}(\cos\theta)\cos\varphi$$
$$+ \sum_{n=1}^{\infty} V_{n,2} P^2_2(\cos\theta_M)P^2_{2n}(\cos\theta)\cos 2\varphi$$
$$+ \sum_{n=1}^{\infty} V_{n,3} P_{2n-2}(\cos\theta), \quad (D3)$$

where the coefficients $V_{n,m}$ ($n = 1 \cdots \infty$, m = 0, 1, 2, 3) are functions of the time t after the flash and $P^i_{2\ell}$ ($\ell = 1 \cdots \infty$, i = 1, 2) are associated Legendre functions. Eq. D can be transformed into four sets of linear equations in the coefficients $V_{n,m}$ ($n = 1 \cdots \infty$, m = 0, 1, 2, 3) by applying Eq. B8 for $k = 2n$ with the definition $P^m_0(\cos\theta) = 0$ for m = 1, 2 and the following properties of Legendre polynomials and associated Legendre functions (Eqs. D4 and D5):

$$\nabla^2_{1M} P^m_2(\cos\theta_Z)\cos m\varphi = -6 P^m_2(\cos\theta_Z)\cos m\varphi$$

$$m = 0, 1, 2 \quad \text{with} \quad P^0_2(\cos\theta_Z) = P_2(\cos\theta_Z), \quad (D4)$$

$$\nabla^2_1 P^m_L(\cos\theta)\cos m\varphi = -L(L + 1)P^m_L(\cos\theta)\cos m\varphi$$

$$m = 0, 1, 2 \quad \text{with} \quad P^0_L(\cos\theta) = P_L(\cos\theta). \quad (D5)$$

Application of Eqs. B8, D4, D5 and the orthogonality and the completeness of the Legendre polynomials and associated Legendre functions allows us to rewrite Eq. D1 as a set of the following four matrix equations for $k = 0, 1, 2, 3$:

$$\frac{d}{dt} V_{n,k} = \sum_{m=1}^{\infty} M_k(n, m)V_{m,k} \quad (n = 1 \cdots \infty), \quad (D6)$$

where all matrix elements $M_k(n, m)$ equal 0 except $M_k(n, n)$, $M_k(n, n+1)$, and $M_k(n+1, n)$ for $k = 0, 1, 2, 3$ and $n = 1 \cdots \infty$:

$$M_0(n, n) = -k_D - 6R_M - (2n - 2)(2n - 1)R$$
$$- \frac{4T(8n^2 - 12n + 3)}{(4n - 5)(4n - 1)} \quad (D7a)$$

$$M_0(n + 1, n) = -\frac{8n(2n - 1)T}{(4n - 1)(4n - 3)} \quad (D7b)$$

$$M_0(n, n + 1) = -\frac{8n(2n - 1)T}{(4n - 1)(4n + 1)} \quad (D7c)$$

$$M_k(n, n) = -k_D - 6R_M - 2n(2n + 1)R$$
$$- \frac{4T(8n^2 + 4n - 1 - 2k^2)}{(4n - 1)(4n + 3)} \quad (k = 1, 2) \quad (D7d)$$

$$M_k(n, n + 1) = -\frac{4T(2n + 2 - k)(2n + 1 + k)}{(4n + 5)(4n + 3)}$$
$$(k = 1, 2) \quad (D7e)$$

$$M_k(n + 1, n) = -\frac{4T(2n + 2 - k)(2n + 1 - k)}{(4n + 3)(4n + 1)}$$
$$(k = 1, 2) \quad (D7f)$$

$$M_3(n, n) = M_0(n, n) + 6R_M \quad (D7g)$$

$$M_3(n + 1, n) = M_0(n + 1, n) \quad (D7h)$$
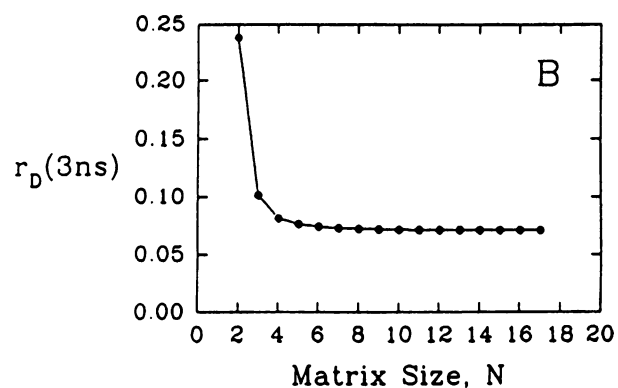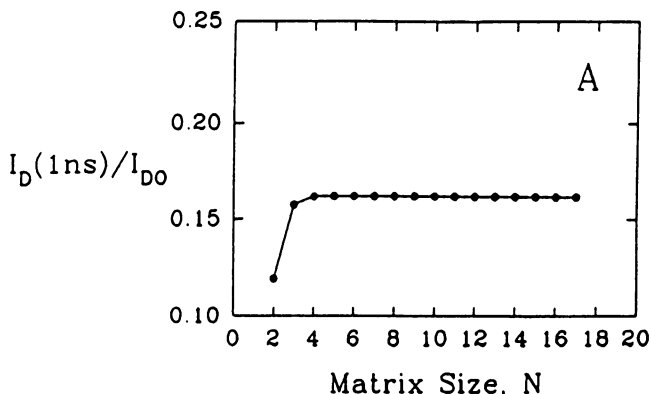
$$M_3(n, n + 1) = M_0(n, n + 1). \quad (D7i)$$

FIGURE 18 Results for I_D and r_D calculated for different cutoff matrices plotted versus the size N of $N \times N$ matrices ($1 < N < 18$). In both panels the following parameter values were used: $k_D = {}^1/_6$ ns^{-1}, $R = 0.1$ ns^{-1}, $T = 3$ ns^{-1}, $R_M = 0$. (A) The donor intensity over its initial value at $t = 1$ ns versus N; (B) the donor anisotropy at $t = 3$ ns is shown. At these times the differences between initial and plateau values were essentially maximal.

Since at the time of the flash $t = 0$, W_D is given by Eqs. D2 and D3, the time 0 values for the coefficients are $V_{2,0} = {}^2\!/_3$, $V_{1,1} = {}^2\!/_9$, $V_{1,2} = {}^1\!/_{18}$, and $V_{1,3} = {}^1\!/_3$ and all other coefficients are equal to 0 at $t = 0$. The intensity of the donor fluorescence response to an extremely short pulse is:

$$I_D(t) = \frac{3I_{D0}}{8\pi} \int_0^{2\pi} \int_0^\pi \int_0^\pi W_D(\theta_Z, \theta, \varphi)$$

$$\times \sin\theta \sin\theta_Z \, d\theta_Z \, d\theta \, d\varphi = 3I_{D0}V_{13}(t), \quad (D8)$$

and the fluorescence anisotropy of the donor is:

$$r_D(t) = \frac{\int_0^{2\pi} \int_0^\pi \int_0^\pi P_2(\cos\theta_D)W_D(\theta_Z, \theta, \varphi) \sin\theta \sin\theta_Z \, d\theta_Z \, d\theta \, d\varphi}{\int_0^{2\pi} \int_0^\pi \int_0^\pi W_D(\theta_Z, \theta, \varphi) \sin\theta \sin\theta_Z \, d\theta_Z \, d\theta \, d\varphi} .$$

$$(D9)$$

Substituting Eq. D2 into $P_2(\cos\theta_D) = \{3(\cos\theta_D)^2 - 1\}/2$, the resulting expression and Eq. D3 into Eq. D9 and evaluating the integrals yields:

$$r_D(t) = \frac{V_{2,0}(t) + 6V_{1,1}(t) + 24V_{1,2}(t)}{25V_{1,3}(t)} . \quad (D10)$$

A series of approximations for $V_{1,3}(t)$, $V_{1,1}(t)$, $V_{1,2}(t)$, and $V_{2,0}(t)$ can be calculated from the eigenvalues and eigenvectors of a series of truncated matrices for the matrices M_0, M_1, M_2, and M_3 in the same way as done in Appendix B:

$$V_{n,k} = \sum_{m=1}^N E_{k,N}(n, m) \exp(\lambda_{k,m}^{(N)} t)$$

$$(n = 1 \cdots N, N = 1 \cdots 17, k = 0 \cdots 3), \quad (D11)$$

where $V_{n,k}$ actually stands for the Nth order approximation to $V_{n,k}$ and $E_{k,N}(n, m)$ is the corresponding nth component of the mth eigenvector with eigenvalue $\lambda_{k,m}^{(N)}$. These eigenvalues are normalized to yield the correct time 0 values for $V_{n,k}$. When I_D and r_D are calculated from Eqs. D8 and D10 using the approximations for $V_{n,k}$ ($n = 1, 2; k = 0 \cdots 3$) of Eq. D11, then for all choices of the parameters convergence is reached before $N = 11$. This convergence is illustrated in Figure 18. Therefore, the results shown in Figures 8 and 10 have been calculated from 11×11 cutoff matrices.

The partial differential equation for the distribution function for the excited acceptors, $W_A = W_A(\theta_Z, \theta, \varphi)$, reads:

$$\frac{\partial}{\partial t} W_A = -k_A W_A + R_M \nabla_{1M}^2 W_A + 4T(\cos\theta)^2 W_D. \quad (D12)$$

Adding Eqs. D1 and D12 yields:

$$\frac{\partial}{\partial t} W_A = -\frac{\partial}{\partial t} W_D - k_D W_D - k_A W_A$$

$$+ R\nabla_1^2 W_D + R_M \nabla_{1M}^2 (W_D + W_A). \quad (D13)$$

Expanding W_A in the same way as W_D in Eq. D3, substituting these expansions into Eq. D13, deriving linear differential equations for the coefficients of the expansions of W_A by equating coefficients on the right to the corresponding ones on the left, simplifying these differential equations by using Eq. D7 and solving them, we find:

$$I_A(t) = \frac{3I_{D0}}{8\pi} \int_0^{2\pi} \int_0^\pi \int_0^\pi W_A(\theta_Z, \theta, \varphi) \sin\theta \sin\theta_Z \, d\theta_Z \, d\theta \, d\varphi$$

$$= \epsilon I_{D0} e^{k_A t} + \frac{4}{5} TI_{D0} \sum_{m=1}^N \{5E_{3,N}(1, m) + 2E_{3,N}(1, m)\} \frac{\exp\{\lambda_{3,m}^{(N)} t\} - \exp\{-k_A t\}}{\lambda_{3,m}^{(N)} + k_A} , \quad (D14)$$

and,

$$r_A(t) = \frac{\int_0^{2\pi} \int_0^\pi \int_0^\pi P_2(\cos\theta_A)W_A(\theta_Z, \theta, \varphi) \sin\theta \sin\theta_Z \, d\theta_Z \, d\theta \, d\varphi}{\int_0^{2\pi} \int_0^\pi \int_0^\pi W_A(\theta_Z, \theta, \varphi) \sin\theta \sin\theta_Z \, d\theta_Z \, d\theta \, d\varphi}$$

$$= \frac{2}{5} e^{-6R_M t} \frac{\epsilon + \frac{4}{5} T \sum_{m=1}^N \{5E_{0,N}(1, m) + 2E_{0,N}(1, m)\} \frac{\exp\{\lambda_{3,m}^{(N)} t + k_A t\} - 1}{\lambda_{3,m}^{(N)} + k_A}}{\epsilon + \frac{4}{5} T \sum_{m=1}^N \{5E_{3,N}(1, m) + 2E_{3,N}(1, m)\} \frac{\exp\{\lambda_{3,m}^{(N)} t + k_A t\} - 1}{\lambda_{3,m}^{(N)} + k_A}} , \quad (D15)$$

where N denotes the size of the cutoff matrix, which should be about 11 in order to ensure precise parameter values.

APPENDIX E

This appendix contains the details of the mathematics for example 3. The numbers at the beginning of the paragraphs refer to the steps in the recipe for model design.

(f) The general matrix equation for $N = 2 \cdots 25$ is given in Eq. E1 below (the special case $N = 4$ is Eq. 15):

$$\frac{d}{dt} x_m = \sum_{l=1}^N B(m, l)x_l \quad (m = 1, \ldots, N) \quad (E1a)$$

$$B(1, 1) = -k_D - Je^{-p_2} - T_1 \quad (E1b)$$

$$B(m, m) = -k_D - J(e^{-p_{m-1}} + e^{-p_{m+1}}) - T_m$$

$$(m = 2, \ldots, N - 1) \quad (E1c)$$

$$B(N, N) = -k_D - Je^{p_{N-1}} - T_N \quad (E1d)$$

$$B(m, m + 1) = Je^{-p_m} \quad (m = 1, \ldots, N - 1) \quad (E1e)$$

$$B(m + 1, m) = Je^{-p_{m+1}} \quad (m = 1, \ldots, N - 1), \quad (E1f)$$

and all other matrix elements are equal to zero. The solution of Eq. E1 with the boundary condition (Eq. 12) reads:

$$x_m = \sum_{l=1}^N C(m, l)e^{\lambda_l t} \quad (m = 1, \ldots, N), \quad (E2)$$

where $C(m, l)$ is the mth component of eigenvector l with eigenvalue λ_l of the matrix in Eq. E1 matching the boundary condition (Eq. 12), i.e., at time $t = 0$,

$$\sum_{l=1}^{N} C(m, l) = e^{-P_m} \Big/ \sum_{m=1}^{N} e^{-P_m}. \tag{E3}$$

The intensity of the donor fluorescence is proportional to the sum of all the probabilities that the donor is excited:

$$I_D = I_{D0} \sum_{m=1}^{N} x_m. \tag{E4}$$

(*h*) The equation for the fractions of molecules with excited acceptors reads:

$$\frac{d}{dt} y_m = T_m x_m + \sum_{l=1}^{N} Y(m, l) y_l, \tag{E5}$$

where $Y(m, l)$ can be obtained from the matrix $B(m, l)$, defined in Eq. E1, by substituting k_A for k_D and 0 for T_m ($m = 1 \cdots N$). The intensity of the acceptor fluorescence is proportional to the sum over all the probabilities that the acceptor is excited:

$$I_A = I_{D0} \sum_{m=1}^{N} y_m. \tag{E6}$$

Adding all the components in Eq. E5 and multiplying with I_{D0} yields the following equation for I_A:

$$\frac{d}{dt} I_A = -k_A I_A + I_{D0} \sum_{m=1}^{N} T_m x_m. \tag{E7}$$

Immediately after the flash I_A equals ϵI_{D0}, where ϵ is the ratio of the direct acceptor fluorescence over the donor fluorescence at the wavelength where the donor is excited. The solution of Eq. E7 with this boundary condition is:

$$I_A = I_{D0} \left[\epsilon e^{-k_A t} + \sum_{m=1}^{N} \sum_{l=1}^{N} T_m C(m, l)(e^{\lambda_l t} - e^{-k_A t})/(\lambda_l + k_A) \right]. \tag{E8}$$

REFERENCES

1. Stryer, L. 1978. Fluorescence energy transfer as a spectroscopic ruler. *Annu. Rev. Biochem.* 47:819–846.

2. Wolber, P. K., and B. S. Hudson. 1979. An analytical solution of the Förster energy transfer problem in two dimensions. *Biophys. J.* 28:197–210.

3. Dewey, T. G., and G. G. Hammes, 1980. Calculation of fluorescence resonance energy transfer on surfaces. *Biophys. J.* 32:1023–1036.

4. Lakowicz, J. R., M. L. Johnson, W. Wiczk, A. Bhat, and R. F. Steiner. 1987. Resolution of a distribution of distances by fluorescence energy transfer and frequency-domain fluorometry. *Chem. Phys. Lett.* 138:587–593.

5. Beechem, J. M., and E. Haas. 1989. Simultaneous determination of intramolecular distance distributions and conformational dynamics by global analysis of energy transfer measurements. *Biophys. J.* 55:1225–1236.

6. Berger, J. W., and J. M. Vanderkooi. 1988. Brownian dynamics simulation of intramolecular energy transfer. *Biophys. Chem.* 30:257–269.

7. Dale, R. E., J. Eisinger, and W. E. Blumberg, 1979. Orientational freedom of molecular probes. The orientation factor in intramolecular energy transfer. *Biophys. J.* 26:161–194 and 30:365.

8. Thomas, D. D., W. F. Carlson, and L. Stryer. 1978. Fluorescence energy transfer in the rapid diffusion limit. *Proc. Natl. Acad. Sci. USA.* 75:5746–5750.

9. Tanaka, F., and N. Mataga. 1979. Theory of time-dependent photo-selection in interacting fixed systems. *Photochem. Photobiol.* 29:1091–1097.

10. Tanaka, F., and N. Mataga. 1982. Dynamic depolarization of interacting fluorophores. Effect of internal rotation and energy transfer. *Biophys. J.* 39:129–140.

11. Piston, D. W., and E. Gratton. 1989. Orientational exchange approach to fluorescence anisotropy decay. *Biophys. J.* 56:1083–1091.

12. Weber, G. 1989. Perrin revisited: parametric theory of the motional depolarization of fluorescence. *J. Phys. Chem.* 93:6069–6073.

13. Haas, E., E. Katchalski-Katzir, and I. Z. Steinberg. 1978. Brownian motion of the ends of oligopeptide chains in solution as estimated by energy transfer between the chain ends. *Biopolymers.* 17:11–31.

14. Van Der Meer, B. W., M. A. Raymer, S. L. Wagoner, R. L. Hackney, J. M. Beechem, and E. Gratton. 1992. Models for fluorescence energy transfer between moving donors and acceptors. *Time-Resolved Laser Spectroscopy in Biochemistry III, Proc. Int. Soc. Opt. Engin. (SPIE)* 1640:220–229.

15. Press, W. H., B. P. Flannery, S. A. Teukolsky, and W. T. Vetterling. 1986. Numerical Recipes (Fortran Version). Cambridge University Press, Cambridge, UK. 635–640.

16. Van Der Meer, B. W. 1992. Rotational jumping model for fluorescence anisotropy from rodlike probes in membranes. *Biophys. J.* 61:181a. (Abstr.)

17. Miers, J. B., J. C. Postelwaite, T. Zyung, S. Chem. G. R. Roemig, X. Wen, D. D. Dlott, and A. Szabo. 1990. Diffusion can explain the nonexponential rebinding of carbon monoxide to protoheme. *J. Chem. Phys.* 93:8771–8776.

18. Cross, A. J., D. H. Waldeck, and G. R. Fleming. 1983. Time resolved polarization spectroscopy: level kinetics and rotational diffusion. *J. Chem. Phys.* 78:6455–6467.

19. Arfken, G. 1985. *Mathematical Methods for Physicists.* Academic Press, New York. 660–680.